

# ***In silico* Proteome analysis of Severe acute respiratory syndrome coronavirus 2 (SARS-CoV-2)**

Chittaranjan Baruah<sup>1\*</sup>, Papari Devi<sup>2</sup>, Dharendra K. Sharma<sup>3</sup>

<sup>1</sup>*Bioinformatics Laboratory (DBT-Star College), P.G. Department of Zoology, Darrang College, Tezpur- 784 001, Assam, India.*

<sup>2</sup>*TCRP Foundation, Guwahati-781005, India*

<sup>3</sup>*School of Biological Science, University of Science and Technology, Meghalaya, India.*

\*Author for correspondence: [chittaranjan\\_21@yahoo.co.in](mailto:chittaranjan_21@yahoo.co.in)

## **ABSTRACT**

Severe acute respiratory syndrome coronavirus 2 (SARS-CoV-2) (2019-nCoV), is a positive-sense, single-stranded RNA coronavirus. The virus is the causative agent of coronavirus disease 2019 (COVID-19) and is contagious through human-to-human transmission. The present study reports sequence analysis, complete coordinate tertiary structure prediction and *in silico* sequence-based and structure-based functional characterization of full SARS-CoV-2 proteome based on the NCBI reference sequence NC\_045512 (29903 bp ss-RNA) which is identical to GenBank entry MN908947 and MT415321. The proteome includes 12 major proteins namely orf1ab polyprotein (includes 15 proteins), surface glycoprotein, ORF3a protein, envelope protein, membrane glycoprotein, ORF6 protein, ORF7a protein, orf7b, ORF8, nucleocapsid phosphoprotein and ORF10 protein. Each protein of orf1ab polyprotein group has been studied separately. A total of 25 polypeptides have been analyzed out of which 15 proteins are not yet having experimental structures and only 10 are having experimental structures with known PDB IDs. Out of 15 newly predicted structures six (6) were predicted using comparative modeling and nine (09) proteins having no significant similarity with so far available PDB structures were modeled using *ab-initio* modeling. The ERRAT and PROCHECK verification revealed that the all-atom model of tertiary structure of high quality and may be useful for structure-based drug designing targets. The study has identified nine major targets (spike protein, envelop protein, membrane protein, nucleocapsid protein, 2'-O-ribose methyltransferase, endoRNase, 3'-to-5' exonuclease, RNA-dependent RNA polymerase and helicase) for which drug design targets can be considered. There are other 16 nonstructural proteins (NSPs), which can also be considered from the drug design perspective. The protein structures are deposited to ModelArchive.

**Key words:** Proteome analysis, orf1ab polyprotein, SARS-CoV-2, 2019-nCoV

## **INTRODUCTION**

Severe acute respiratory syndrome coronavirus 2 (SARS-CoV-2), is a positive-sense, single-stranded RNA coronavirus, which is a major source of disaster in the 21<sup>st</sup> century. The virus is the causative agent of coronavirus disease 2019 (COVID-19) and is contagious through human-to-human transmission. Coronaviruses (CoVs) have a single-stranded RNA genome (size range between 26.2 and 31.7 kb, positive sense), covered by an enveloped structure (Yang *et al.*, 2006). A typical CoV contains at least six ORFs in its genome. SARS-CoV-2 is the seventh coronavirus that is known to cause human disease. Coronaviruses (CoVs) are a group of large and enveloped viruses with positive-sense, single-stranded RNA genomes (Lai *et al.*, 2007; Lu and Liu, 2012). Previously identified human CoVs that cause human disease include the alphaCoVs hCoV-NL63 and hCoV-229E and the betaCoVs HCoV-OC43, HKU1, severe acute respiratory syndrome CoV (SARS-CoV), and Middle East respiratory syndrome CoV

(MERS-CoV) (Lu *et al.*, 2015). Among these seven strains, three strains proved to be highly pathogenic (SARS-CoV, MERS-CoV, and 2019-nCoV), which caused endemic of severe CoV disease (Paules *et al.*, 2020). The viruses can be classified into four genera: alpha, beta, gamma, and deltaCoVs (Woo *et al.*, 2009). Both alphaCoVs and the betaCoVs HCoV-OC43 and HKU1 cause self-limiting common cold-like illnesses (Chiu *et al.*, 2005; Jean *et al.*, 2013). However, SARS-CoV and MERS-CoV infection can result in life-threatening disease and have pandemic potential. SARS-CoV-2 is responsible for the infection with special reference to the involvement of the respiratory tract (both lower and upper respiratory tract), e.g., common cold, pneumonia, bronchiolitis, rhinitis, pharyngitis, sinusitis, and other system symptoms such as occasional watery and diarrhea (Chang *et al.*, 2016; Paules *et al.*, 2020).

The current classification of coronaviruses recognizes 39 species in 27 subgenera, five genera and two subfamilies that belong to the family *Coronaviridae*, suborder *Coronovirineae*, order *Nidovirales* and realm *Riboviria* (Ziebuhr *et al.*, 2017; Siddell *et al.*, 2019; Ziebuhr *et al.*, 2019). The family classification and taxonomy are developed by the *Coronaviridae* Study Group (CSG), a working group of the ICTV (de Groot *et al.*, 2012). To accommodate the wide spectrum of clinical presentations and outcomes of infections caused by SARS-CoV-2 (ranging from asymptomatic to severe or even fatal in some cases) (Huang *et al.*, 2020), the WHO recently introduced a rather unspecific name (coronavirus disease 19, also known as COVID-19 (World Health Organization, 2020) to denote this disease. Whole-genome sequencing results showed that the causative agent was a novel coronavirus that was initially named 2019-nCoV by the World Health Organization (WHO) (Wu *et al.*, 2020; Zhou *et al.*, 2020; Zhu *et al.*, 2020). Later, the International Committee on Taxonomy of Viruses (ICTV) officially designated the virus SARS-CoV-2 (*Coronaviridae* Study Group of the International Committee on Taxonomy of Viruses, 2020), although many virologists argue that HCoV-19 is more appropriate (Jiang *et al.*, 2020).

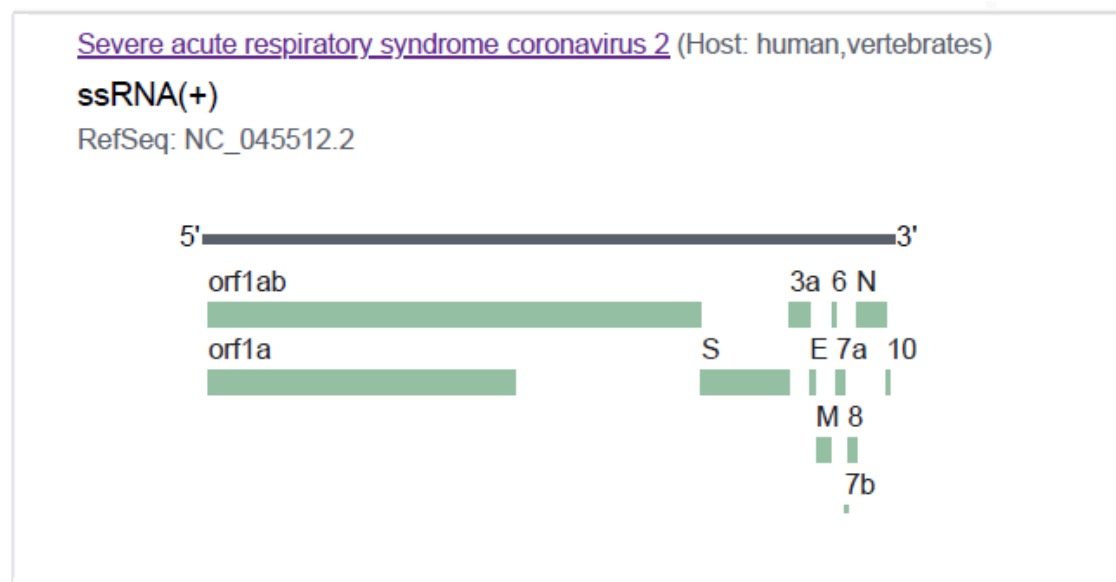


**Figure 1.** The structure of SARS-CoV-2 reference genome (NC\_045512.2) used in the present study. The genome size is 29.9 Kb with GC% 38.0 and 11 genes which encodes 12 major proteins. SARS-CoV-2 has four structural proteins: the E and M proteins, which form the viral envelope; the N protein, which binds to the virus's RNA genome; and the S protein, which binds to human receptors. (Source: NCBI)

There is lack of specific drugs to treat an attack, which is an urgent need at this current point of time. Understanding the complete proteome of SARS-CoV-2 is the need of the hour. The major structural proteins namely

the E and M proteins, which form the viral envelope; the N protein, which binds to the virus's RNA genome; and the S protein, which binds to human receptors, may serve an important role from vaccine development or drug design perspectives. The nonstructural proteins get expressed as two long polypeptides, the longer of which gets chopped up by the virus's main protease. This group of proteins includes the main protease (Nsp5) and RNA polymerase (Nsp12) has equal importance for structure based drug designing. In this regard, the present study reports sequence analysis and structure prediction (both Comparative and *ab-initio* modeling) of full SARS-CoV-2 proteome based on the NCBI reference sequence NC\_045512 (29903 bp ss-RNA) which is identical to GenBank entry MN908947 and MT415321 (Table 1).

The viral genome encodes 29 proteins (*Nature* DOI: 10.1038/s41433-020-0790-7). In the present analysis 25 proteins of NCBI reference sequence NC\_045512 (Figure 1) (including 15 proteins of orf1ab) from the proteome have been analyzed out of which 15 proteins are not yet having experimental structures and 10 are having experimental structures with known PDB IDs. Out of 15 predicted structures six (6) proteins namely NSP6, Surface glycoprotein, Envelope protein, ORF7a, ORF8 and Nucleoproteins were predicted using comparative modeling and nine (09) proteins namely NSP1, NSP2, NSP3, NSP4, ORF3a, Membrane protein, ORF6, ORF7b and ORF10 having no significant similarity with so far available PDB structures were modeled using *ab-initio* modeling.

## MATERIALS AND METHODS

### *Acquisition and analysis of sequences*

The sequence of full SARS-CoV-2 proteome based on the NCBI reference sequence **NC\_045512 (29903 bp ss-RNA)** along with GenBank entry MN908947 and **MT415321** were analyzed (**Table 1**). A total of 25 proteins from the proteome have been analyzed out of which 15 proteins are not yet having experimental structures based on BLASTp ([Altschul et al., 1997](#)) and FASTA ([Pearson, 1991](#)) searches.

### *Three-dimensional structure prediction (Comparative and ab-initio modeling)*

Out of the 25 polypeptide chains, ten (10) are having experimental structures with PDB IDs. Therefore, three dimensional structure predictions were carried out for fifteen (15) proteins for which complete 3D co-ordinate files are yet not available. BlastP and FASTA searches were performed independently with PDB to know the existing PDB structure, for obtaining a suitable template for Comparative modeling and to select the proteins for which *ab-initio* modeling is required (**Table 2**). The significance of the BLAST results was assessed by expect values (e-value) generated by BLAST family of search algorithm and query coverage. Six (6) proteins namely NSP6, Surface glycoprotein, Envelope protein, ORF7a, ORF8 and Nucleoproteins were predicted using comparative modeling using Modeller9.23 program ([Webb and Sali, 2016](#)) and Baker Rosetta Server (<https://rosetta.bakerlab.org/>); nine (09) proteins namely NSP1, NSP2, NSP3, NSP4, ORF3a, Membrane protein, ORF6, ORF7b and ORF10 having no significant similarity with so far available PDB structures were modeled using *ab-initio* modeling using Baker Rosetta Server (<https://rosetta.bakerlab.org/>). The loop regions were modeled using ModLoop server ([Fiser and Sali, 2003](#)). The final 3D structures with complete coordinates were obtained by optimization of a molecular probability density function (pdf) of Modeller ([Eswar et al., 2006](#)). The molecular pdf for modelling was optimized with the variable target function procedure in Cartesian space that employed the method of conjugate gradients and molecular dynamics with simulated annealing (Sali and Blundell, 1993). The computational protein structures were verified by using Global and local (per-residue) quality estimates using ProQ3, ModFOLD6-TS, QMEANDisCo 4.0.0 ([Haas et al., 2019](#)). After fruitful verification, the coordinate files were successfully deposited to

ModelArchive (<https://www.modelarchive.org>) All the graphic presentations of the 3D structures were prepared using Chimera version 1.8.1 (Pettersen *et al.*, 2004).

### Proteomics analysis

The proteomics analyses were carried out using ExPASy proteomic tools (<https://www.expasy.org/tools>). The Data mining, sequence analyses for physico-chemical parameters of SARS-CoV-2 proteomes were computed using ProtParam (Gasteiger *et al.*, 2005) and BioEdit. The important calculations for the amino acid composition, atomic composition, theoretical pI, molecular weight, Formula, extinction coefficients, half-life, instability index, aliphatic index, hydrophobicity, charge vs. pH were carried out under sequence analysis (Table 3).

The sequence based functional annotation have been carried out for SARS-CoV-2 proteome in the sequence database, using Pfam ([pfam.sanger.ac.uk/](http://pfam.sanger.ac.uk/)), GO ([www.geneontology.org/](http://www.geneontology.org/)), KEGG database ([www.genome.jp/kegg/](http://www.genome.jp/kegg/)). ProFunc server (Laskowski *et al.*, 2005) was used to identify the likely biochemical function of proteins from the predicted three-dimensional structure. Hmmer version 3.3 (Finn *et al.*, 2011), PFam, PROSITE, PRINTS, ProDom, InterProScan were used for functional characterization. MOLE 2.0 (Sehna *et al.*, 2013) was used for advanced analysis of biomacromolecular channels.

## RESULTS AND DISCUSSION

The ORF1ab polyprotein is the largest protein (7096 amino acids; 794.017kDa) out of SARS-CoV-2. It is rich in Leucine (9.41%) and Valine (8.43%). The protein has theoretical Isoelectric point (pI) 6.32, Instability index 33.31, Aliphatic index 86.87 and Grand average of hydropathicity - 0.070 (Figure 2a; Table 3). It is a multifunctional protein involved in the transcription and replication of viral RNAs. It contains the proteinases responsible for the cleavages of the polyprotein.

InterPro classification of protein families ORF1ab polyprotein belongs to Non-structural protein NSP1, betacoronavirus (IPR021590) protein family. The biological process associated with ORF1ab protein includes-viral genome replication (GO :0019079), viral protein processing (GO :0019082), proteolysis (GO :0006508), transcription, DNA-templated (GO :0006351) and viral RNA genome replication (GO :0039694).

The molecular functions associated are zinc ion binding (GO :0008270), RNA binding (GO :0003723), omega peptidase activity (GO :0008242), cysteine-type endopeptidase activity (GO :0004197), transferase activity (GO :0016740), single-stranded RNA binding (GO :0003727), cysteine-type peptidase activity (GO :0008234), RNA-directed 5'-3' RNA polymerase activity (GO :0003968), ATP binding (GO :0005524) and nucleic acid binding (GO :0003676).

Hits for all PROSITE (release 2020\_02) motifs on sequence of ORF1ab (YP\_009724389-1) has detected 8 hits (Table 4)– (i)Peptidase family C16 domain profile : PS51124| PEPTIDASE\_C16 (profile) Peptidase family C16 domain profile :1634 - 1898: score=60.973; (ii) Coronavirus main protease (M-pro) domain profile : PS51442|M\_PRO (profile) Coronavirus main protease (M-pro) domain profile : 3264 - 3569: score=154.193; (iii) RdRp of positive ssRNA viruses catalytic domain profile : PS50507|RDRP\_SSRNA\_POS (profile) RdRp of positive ssRNA viruses catalytic domain profile : 5004 - 5166: score=8.290; (iv) Coronaviridae zinc-binding (CV ZBD) domain profile : PS51653| CV\_ZBD (profile) Coronaviridae zinc-binding (CV ZBD) domain profile : 5325 - 5408: score=33.035; (v) (+)RNA virus helicase core domain profile : PS51657|PSRV\_HELICASE (profile) (+)RNA virus helicase core domain profile : 5581 - 5932: score=27.299; (vi) Carbamoyl-phosphate synthase

subdomain signature 2 : PS00867|CPSASE\_2 (pattern) Carbamoyl-phosphate synthase subdomain signature 2 : 2061 - 2068: [confidence level: (-1)]; vii) Lipocalin signature : PS00213| LIPOCALIN (pattern) Lipocalin signature : 4982 - 4993: [confidence level: (-1)] .

The ORF1a polyprotein (Length = 4405 amino acids;Molecular Weight = 489.963kDa) is also rich in Leucine (9.88%) and Valine (8.42%). ORF1a polyprotein has theoretical Isoelectric point (pI) 6.04, Instability index 34.92, Aliphatic index 88.87 and Grand average of hydropathicity - 0.023 (Figure 2B; Table 3).

InterPro classification of protein families ORF1a polyprotein belongs to Non-structural protein NSP1, betacoronavirus (IPR021590) family. It is involved in biological processes- viral genome replication (*GO*: 0019079), viral protein processing (*GO*: 0019082) and proteolysis (*GO*: 0006508).

The molecular functions of ORF1a polyprotein are omega peptidase activity (*GO*: 0008242), cysteine-type endopeptidase activity (*GO*: 0004197), transferase activity (*GO*: 0016740), RNA binding (*GO*: 0003723), nucleic acid binding (*GO*: 0003676), zinc ion binding (*GO*: 0008270), cysteine-type peptidase activity (*GO*: 0008234), RNA-directed 5'-3' RNA polymerase activity (*GO*: 0003968), and single-stranded RNA binding (*GO*: 0003727).

Hits for all PROSITE (release 2020\_02) motifs on sequence of ORF1a (YP\_009725295-1) has found 4 hits (Table 4)- (i) Macro domain profile :PS51154|MACRO (profile) Macro domain profile :1025 - 1194: score=18.014; (ii) Peptidase family C16 domain profile : PS51124|PEPTIDASE\_C16 (profile) Peptidase family C16 domain profile :1634 - 1898: score=60.973; (iii) Coronavirus main protease (M-pro) domain profile : PS51442|M\_PRO (profile) Coronavirus main protease (M-pro) domain profile : 3264 - 3569: score=154.193; (iv)Carbamoyl-phosphate synthase subdomain signature 2: >PS00867|CPSASE\_2 (pattern) Carbamoyl-phosphate synthase subdomain signature 2 : 2061 - 2068: [confidence level: (-1)].

The ORF1ab polyprotein is protein complex of 15 proteins namely NSP1, NSP2, NSP3, NSP4, 3C-like proteinase, NSP6, NSP7, NSP8, NSP9, NSP10, RNA-dependent RNA polymerase, Helicase, 3'-to-5' exonuclease, EndoRNase and 2'-O-ribose methyltransferase. Orf1ab polyprotein is a multifunctional protein involved in the transcription and replication of viral RNAs. Predicted functions of SARS-CoV-2 proteome with respective ProFunc score is listed in Table 4).

## 1. Leader protein (NSP1) (PF11501)

Non-structural protein NSP1 (IPR021590) is the N-terminal cleavage product from the viral replicase that mediates RNA replication and processing (Almeida *et al.*, 2007). ProMotif results revealed that the structure of NSP1 protein has 2 sheets, 5 beta hairpins, 4 beta bulges, 7 strands, 5 helices, 1 helix-helix interacts, 22 beta turns and 3 gamma turns (Figure 3 A). Physicochemical parameter analysis computed that NSP1 has theoretical Isoelectric point (pI) 5.36, Instability index 28.83, Aliphatic index 89.72 and Grand average of hydropathicity - 0.378 (Table 3).

NSP1 binds to the 40S ribosomal subunit and inhibits translation, and it also induces a template-dependent endonucleolytic cleavage of host mRNAs (Kamitani *et al.*, 2009). Structurally, NSP1 consists of a mixed parallel/antiparallel 6-stranded beta barrel with an alpha helix covering one end of the barrel and another helix alongside the barrel (Almeida *et al.*, 2007). NSP1 also suppresses the host innate immune functions by inhibiting type I interferon expression and host antiviral signaling pathways (Almeida *et al.*, 2007).

## 2. Non-structural protein 2 (nsp2)

ProMotif results revealed that the structure of NSP2 has 2 sheets, 2 beta hairpins, 1 beta bulge, 4 strands;



23 helices; 15 helix-helix interactions; 40 beta turns; 10 gamma turns; 1 disulphide (Figure 3B). NSP2 has theoretical Isoelectric point (pI) 6.25, Instability index 36.06, Aliphatic index 88.93 and Grand average of hydropathicity - 0.062 (Table 3). This protein may play a role in the modulation of host cell survival signaling pathway by interacting with host PHB and PHB2.

### 3. Non-structural protein 3 (NSP3)

ProMotif results revealed that the structure of NSP3 has 6 sheets, 10 beta hairpins, 6 beta bulges, 23 strands, 139 helices, 130 helix-helix interactions, 169 beta turns, 45 gamma turns, 6 disulphides (Figure 3C). NSP3 has theoretical Isoelectric point (pI) 5.56, Instability index 36.56, Aliphatic index 86.22 and Grand average of hydropathicity - 0.175 (Table 3).

Biological Process of NSP3 is proteolysis (GO: 0006508) and it involves in molecular function such as single-stranded RNA binding (GO: 0003727), cysteine-type peptidase activity (GO: 0008234), RNA-directed 5'-3' RNA polymerase activity (GO: 0003968) and nucleic acid binding (GO: 0003676).

### 4. Non-structural protein 4 (NSP4)

ProMotif results revealed that the structure of NSP4 has 5 sheets, 6 beta hairpins, 3 beta bulges, 11 strands, 16 helices, 20 helix-helix interactions, 41 beta turns, 6 gamma turns (Figure 3D). NSP4 has theoretical Isoelectric point (pI) 7.16, Instability index 34.09, Aliphatic index 95.50 and Grand average of hydropathicity - 0.343 (Table 3). NSP4 Participates in the assembly of virally-induced cytoplasmic double-membrane vesicles necessary for viral replication. This C-terminal domain (InterPro entry IPR032505) is predominantly alpha-helical, which may be involved in protein-protein interactions (Manolaridis *et al.*, 2009)

### 5. 3C-like protein

ProMotif results revealed that the structure of 3C-like proteinase has 2 sheets, 7 beta hairpins, 7 beta bulges, 13 strands, 8 helices, 9 helix-helix interactions, 28 beta turns and 2 gamma turns. 3C-like proteinase has theoretical Isoelectric point (pI) 5.95, Instability index 27.65, Aliphatic index 82.12 and Grand average of hydropathicity - 0.019 (Table 3).

The biological process of 3C-like proteinase is the viral protein processing (GO :0019082). It resembles Peptidase\_C30 (PF05409) family which corresponds to Merops family C30. These peptidases are involved in viral polyprotein processing in replication.

### 6. Non-structural protein 6 (NSP6)

ProMotif results revealed that the structure of NSP6 has 1 sheet, 1 beta hairpin, 2 strands, 14 helices, 31 helix-helix interactions, 9 beta turns, 2 gamma turns (Figure 3E). NSP6 has theoretical Isoelectric point (pI) 9.11, Instability index 22.94, Aliphatic index 111.55 and Grand average of hydropathicity - 0.790 (Table 3). Nsp6 may play a role in the initial induction of autophagosomes from host's endoplasmic reticulum.

It has been reported that NS6 can increase the cellular gene synthesis and it can also induce apoptosis through Jun N-terminal kinase and Caspase-3 mediated stress (Cheng *et al.*, 2015). This protein can modulate host antiviral responses by inhibiting synthesis and signalling of interferon-beta (IFN-beta) via two complementary pathways. One involves NS6 interaction with host N-Myc (and STAT) interactor (Nmi) protein inducing its degradation via ubiquitin proteasome pathway, suppressing Nmi enhanced IFN signalling. The other pathway suppresses the translocation of signal transducer and activator of transcription 1 (STAT1) and downstream IFN signalling (Cheng *et al.*, 2015)

## 7. Non-structural protein 7 (NSP7)

NSP7 is predominantly a alpha helical structure. ProMotif results revealed that the structure of NSP7 has 3 helices, 7 helix-helix interactions and 3 beta turns (PDB ID 7BV1\_C). NSP7 has theoretical Isoelectric point (pI) 5.18, Instability index 51.97, Aliphatic index 117.35 and Grand average of hydropathicity -0.199 (Table 3). NSP7 may have the function in activating RNA-synthesizing activity and it forms a hexadecamer with nsp8 that may also participate in viral replication by acting as a primase. Molecular Function predicted by InterPro scan has predicted its molecular functions as omega peptidase activity (GO :0008242), cysteine-type endopeptidase activity (GO :0004197) and transferase activity (GO :0016740). NSP 7 belongs to nsp7 (PF08716). nsp7 (non structural protein 7) has been implicated in viral RNA replication.

## 8. Non-structural protein 8 (NSP8)

ProMotif results revealed that the structure of NSP8 has 2 sheets, 2 beta hairpins, 1 beta bulge, 5 strands, 5 helices, 6 helix-helix interactions, 13 beta turns, 1 gamma turn (PDB ID 7BV1\_B). NSP8 has theoretical Isoelectric point (pI) 6.58, Instability index 37.78, Aliphatic index 88.33 and Grand average of hydropathicity -0.192 (Table 3). It forms a hexadecamer with nsp7 that may participate in viral replication by acting as a primase. Molecular Functions of NSP8 are scanned as transferase activity (GO: 0016740), cysteine-type endopeptidase activity (GO :0004197) and omega peptidase activity (GO :0008242).

NSP alone as a monomer structure may not be biologically relevant as it forms a hexadecameric supercomplex with nsp7. The dimensions of the central channel and positive electrostatic properties of the cylinder imply that it confers processivity on RNA-dependent RNA polymerase (Zhai *et al.*, 2005).

## 9. Non-structural protein 9 (NSP9)

ProMotif results revealed that the structure of Nsp9 has 2 sheets, 5 beta hairpins, 4 beta bulges, 7 strands 1 helix, 11 beta turns. NSP9 has theoretical Isoelectric point (pI) 9.10, Instability index 34.17, Aliphatic index 82.92 and Grand average of hydropathicity -0.227 (Table 3). May participate in viral replication by acting as a ssRNA-binding protein. NSP9 may have biological processes viral genome replication (GO: 0019079) and molecular function RNA binding (GO: 0003723). The NSP9 (PF08710) is a single-stranded RNA-binding viral protein likely to be involved in RNA synthesis (Egloff *et al.*, 2004). Its structure comprises of a single beta barrel (Campanacci *et al.*, 2003).

## 10. Non-structural protein 10 (NSP10)

ProMotif results revealed that the structure of NSP10 has 2 sheets, 1 beta hairpin, 5 strands, 6 helices, 3 helix-helix interactions, 13 beta turns, 1 gamma turn. NSP10 has theoretical Isoelectric point (pI) 6.29, Instability index 34.56, Aliphatic index 61.80 and Grand average of hydropathicity -0.068 (Table 3). It plays an essential role in viral mRNAs cap methylation.

The NSP 10 (PF09401) have biological process - viral genome replication (GO: 0019079) and Molecular function- RNA binding (GO: 0003723), zinc ion binding (GO: 0008270). A cluster of basic residues on the protein surface suggests a nucleic acid-binding function. Interacting selectively and non-covalently with an RNA molecule or a portion thereof. NSP10 contains two zinc binding motifs and forms two anti-parallel helices which are stacked against an irregular beta sheet (Joseph *et al.*, 2006). Nsp10 binds to nsp16 through an activation surface area in nsp10, and the resulting complex exhibits RNA cap (nucleoside-2'-O)-methyltransferase activity.

## 11. RNA-dependent RNA polymerase (Pol/RdRp)

ProMotif results revealed that the structure of RNA-dependent RNA polymerase has 8 sheets, 8 beta hairpins, 1 psi loop, 2 beta bulges, 22 strands, 41 helices, 58 helix-helix interactions, 91 beta turns and 16 gamma turns. It is associated with replication and transcription of the viral RNA genome. RNA-dependent RNA polymerase has theoretical Isoelectric point (pI) 6.14, Instability index 28.32, Aliphatic index 78.43 and Grand average of hydropathicity -0.224 (Table 3).

The biological process of Pol/RdRp (*Corona\_RPol\_N*\_PF06478) is associated with transcription, DNA-templated (GO: 0006351), and viral RNA genome replication (GO :0039694). The molecular functions are predicted as RNA-directed 5'-3' RNA polymerase activity (GO :0003968), RNA binding (GO :0003723) and ATP binding (GO :0005524). Coronavirus RPol N-terminus family covers the N-terminal region of the coronavirus RNA-directed RNA polymerase. The nsp7 and nsp8 activate and confer processivity to the RNA-synthesizing activity of Pol (Kirchdoerfer and Ward, 2019).

## 12. Helicase

ProMotif results revealed that the structure of Helicase has 8 sheets, 1 beta alpha beta unit, 7 beta hairpins, 5 beta bulges, 26 strands, 19 helices, 16 helix-helix interactions, 92 beta turns, 15 gamma turns. Helicase has theoretical Isoelectric point (pI) 8.66, Instability index 33.31, Aliphatic index 84.49 and Grand average of hydropathicity -0.096 (Table 3).

Helicase protein has molecular functions- zinc ion binding (GO: 0008270) and ATP binding (GO: 0005524). Multi-functional protein Helicase is with a zinc-binding domain in N-terminus displaying RNA and DNA duplex-unwinding activities with 5' to 3' polarity. Activity of helicase is dependent on magnesium (By Similarity).



### 13. 3'-to-5' exonuclease

ProMotif results revealed that the structure of 3'-to-5' exonuclease has 6 sheets, 8 beta hairpins, 3 beta bulges, 23 strands, 13 helices, 10 helix-helix interactions, 60 beta turns. 3'-to-5' exonuclease has theoretical Isoelectric point (pI) 7.80, Instability index 28.85, Aliphatic index 78.96 and Grand average of hydropathicity -0.134 (Table 3). The two possible activities of 3'-to-5' exonuclease (NSP14) include exoribonuclease activity acting on both ssRNA and dsRNA in a 3' to 5' direction and a N7-guanine methyltransferase activity.

### 14. endoRNase/ nsp15

ProMotif results revealed that the structure of endoRNase (NSP15) has 7 sheets, 1 beta alpha beta unit, 9 beta hairpins, 6 beta bulges, 21 strands, 10 helices, 8 helix-helix interactions, 37 beta turns and 2 gamma turns. endoRNase (NSP15) has theoretical Isoelectric point (pI) 5.06, Instability index 36.28, Aliphatic index 95.09 and Grand average of hydropathicity -0.076 (Table 3). endoRNase is a Mn(2+)-dependent, uridylylate-specific enzyme, which leaves 2'-3'-cyclic phosphates 5' to the cleaved bond.

### 15. 2'-O-ribose methyltransferase

ProMotif results revealed that the structure of 2'-O-ribose methyltransferase (NSP16) has 3 sheets, 3 beta alpha beta units, 1 beta hairpin, 2 beta bulges, 12 strands, 12 helices, 6 helix-helix interactions, 15 beta turns and 4 gamma turns. 2'-O-ribose methyltransferase has theoretical Isoelectric point (pI) 7.59, Instability index 26.11, Aliphatic index 90.64 and Grand average of hydropathicity -0.086 (Table 3).

2'-O-ribose methyltransferase belongs to *NSP16* family (PF06460). The SARS-CoV RNA cap SAM-dependent (nucleoside-2'-O-)-methyltransferase (2'-O-MTase) is a heterodimer comprising SARS-CoV nsp10 and nsp16. Nsp16 adopts a typical fold of the S-adenosylmethionine-dependent methyltransferase (SAM) family as defined initially for the catechol O-MTase but it lacks several elements of the canonical MTase fold, such as helices B and C. The 2'-O-ribose methyltransferase (nsp16) topology matches those of dengue virus NS5 N-terminal domain and of vaccinia virus VP39 MTases (Chen *et al.*, 2011).

### 16. Surface glycoprotein (spike glycoprotein)

ProMotif results revealed that the structure of Surface glycoprotein (**spike glycoprotein**) has 13 sheets, 18 beta hairpins, 18 beta bulges, 52 strands, 22 helices, 29 helix-helix interactions, 76 beta turns, 16 gamma turns and 12 disulphides (Figure 3F). Surface glycoprotein (Length = 1273 amino acids; Molecular Weight = 141.113kDa) is rich in Leucine (8.48%) and Serine (7.78 %). Surface glycoprotein has theoretical Isoelectric point (pI) 6.32, Instability index 32.86, Aliphatic index 84.67 and Grand average of hydropathicity -0.077 (Figure 2C; Table 3).

Surface glycoprotein involves in two important biological processes i.e. receptor-mediated virion attachment to host cell (GO: 0046813) and membrane fusion (GO: 0061025). **Spike protein S1** attaches the virion to the cell membrane by interacting with host receptor, initiating the infection. Binding to human ACE2 and CLEC4M/DC-SIGNR receptors and internalization of the virus into the endosomes of the host cell induces

conformational changes in the S glycoprotein. **Spike protein S2** mediates fusion of the virion and cellular membranes by acting as a class I viral fusion protein. **Spike protein S2'** Acts as a viral fusion peptide which is unmasked following S2 cleavage occurring upon virus endocytosis. It is a part of cellular components viral envelope (GO: 0019031) and integral component of membrane (GO: 0016021).

## 17. ORF3a protein

ProMotif results revealed that the structure of ORF3a protein (**Papain-like protease**) has 7 sheets, 8 beta hairpins, 2 beta bulges, 15 strands, 6 helices, 3 helix-helix interactions, 28 beta turns, 2 gamma turns and 1 disulphide (Figure 3G). ORF3a protein (Molecular Weight = 31121.29 Daltons) is rich in Leucine (10.91%), Valine (9.09%), Threonine (8.73%) and Serine (8.00%). ORF3a protein has theoretical Isoelectric point (pI) 5.55, Instability index 32.96, Aliphatic index 103.42 and Grand average of hydropathicity 0.275 (Figure 2D; Table 3).

The protein belongs to family Protein 3a, betacoronavirus (IPR024407). Protein 3a encoded by Orf3/3a, also known as X1, which forms homotetrameric potassium, sodium or calcium sensitive ion channels (viroporin) and may modulate virus release. It has also been shown to up-regulate expression of fibrinogen subunits FGA, FGB and FGG in host lung epithelial cells (Shen *et al.*, 2005; Lu *et al.*, 2006).

3a protein is a pro-apoptosis-inducing protein. It localises to the endoplasmic reticulum (ER)-Golgi compartment. SARS-CoV causes apoptosis of infected cells through NLRP3 inflammasome activation, as ORF3a is a potent activator of the signals required for this activation, pro-IL-1 $\beta$  gene transcription and protein maturation. This protein also promotes the ubiquitination of apoptosis-associated speck-like protein containing a caspase recruitment domain (ASC) mediated by its interaction with TNF receptor-associated factor 3 (TRAF3). The expression of ORF3a induces NF-kappa B activation and up-regulates fibrinogen secretion with the consequent high cytokine production (Yu *et al.*, 2004; Lu *et al.*, 2006).

Another apoptosis mechanism described for this protein is the activation of the PERK pathway of unfolded protein response (UPR), which causes phosphorylation of eIF2 $\alpha$  and leads to reduced translation of cellular proteins as well as the activation of pro-apoptotic downstream effectors (i.e ATF4, CHOP) (Minakshi *et al.*, 2009).

## 18. Envelope protein (E protein)

ProMotif results revealed that the structure of Envelope protein (E protein) has 4 helices, 2 helix-helix interactions and 3 beta turns (Figure 3H). Envelope protein (Molecular Weight = 8364.59 Daltons) is rich in Leucine (18.67%) and Valine (17.33%). Envelope protein has theoretical Isoelectric point (pI) 8.57, Instability index 38.68, Aliphatic index 144.00 and Grand average of hydropathicity 1.128 (Figure 2E; Table 3).

The Envelope protein belongs to protein family Envelope small membrane protein, coronavirus (IPR003873) and Envelope small membrane protein, betacoronavirus (IPR043506). It plays a central role in virus morphogenesis and assembly. Biological Process of Envelope protein is pore formation by virus in membrane of host cell (GO: 0039707).

E proteins are well conserved among Coronavirus strains. They are small, integral membrane proteins involved in several aspects of the virus' life cycle, such as assembly, budding, envelope formation, and

pathogenesis (Schoeman and Fielding, 2019). E protein acts as a viroporin by oligomerizing after insertion in host membranes to create a hydrophilic pore that allows ion transport (Madan *et al.*, 2005; Surya *et al.*, 2015).

SARS-CoV E protein forms a  $\text{Ca}^{2+}$  permeable channel in the endoplasmic reticulum Golgi apparatus intermediate compartment (ERGIC)/Golgi membranes. The E protein ion channel activity alters  $\text{Ca}^{2+}$  homeostasis within cells boosting the activation of the NLRP3 inflammasome, which leads to the overproduction of IL-1 $\beta$ . SARS-CoV overstimulates the NF-kappaB inflammatory pathway and interacts with the cellular protein syntenin, triggering p38 MARK activation. These signalling cascades result in exacerbated inflammation and immunopathology (Nieto-Torres *et al.*, 2015).

## 19. Membrane glycoprotein (M protein)

ProMotif results revealed that the structure of Membrane glycoprotein 9 helices, 8 helix-helix interacts, 28 beta turns and 11 gamma turns (Figure 3I). Membrane glycoprotein (Molecular Weight = 25145.16 Daltons) Leucine (15.77%) and Isoleucine (9.01%). Membrane glycoprotein has theoretical Isoelectric point (pI) 9.51, Instability index 39.14, Aliphatic index 120.86 and Grand average of hydropathicity 0.446 (Figure 2F; Table 3).

Biological process of M protein is viral life cycle (GO: 0019058) ; includes attachment and entry of the virus particle, decoding of genome information, translation of viral mRNA by host ribosomes, genome replication, and assembly and release of viral particles containing the genome.

M protein is a component of the viral envelope that plays a central role in virus morphogenesis and assembly via its interactions with other viral proteins. Protein family membership of M protein includes FM matrix/glycoprotein, coronavirus (IPR002574). This family consists of various coronavirus matrix proteins which are transmembrane glycoproteins (Armstrong *et al.*, 1984).

The membrane (M) protein is the most abundant structural protein and defines the shape of the viral envelope. It is also regarded as the central organiser of coronavirus assembly, interacting with all other major coronaviral structural proteins. M proteins play a critical role in protein-protein interactions (as well as protein-RNA interactions) since virus-like particle (VLP) formation in many CoVs requires only the M and envelope (E) proteins for efficient virion assembly (Ujike and Taguch, 2015).

Interaction of spike (S) with M is necessary for retention of S in the ER-Golgi intermediate compartment (ERGIC)/Golgi complex and its incorporation into new virions, but dispensable for the assembly process. Binding of M to nucleocapsid (N) proteins stabilises the nucleocapsid (N protein-RNA complex), as well as the internal core of virions, and, ultimately, promotes completion of viral assembly. Together, M and E protein make up the viral envelope and their interaction is sufficient for the production and release of virus-like particles (VLPs) (Schoeman and Fielding, 2019).

## 20. ORF6 protein

ProMotif results revealed that the structure of ORF6 protein has 3 helices, 1 helix-helix interact, 2 beta turns and 1 gamma turn (Figure 3 J). ORF6 protein (Molecular Weight = 7272.15 Daltons) is rich in Isoleucine (16.39%) and Leucine (13.11%). ORF6 protein has theoretical Isoelectric point (pI) 4.60, Instability index 31.16, Aliphatic index 130.98 and Grand average of hydropathicity 0.233 (Figure 2G; Table 3).

The ORF6 protein belongs to the protein family Non-structural protein NS6, betacoronavirus (IPR022736). Proteins in this family are typically between 42 to 63 amino acids in length, highly conserved among SARS-related coronaviruses (Geng *et al.*, 2005).

## 21. ORF7a protein

Protein 7a (X4 like protein) is a non-structural protein which is dispensable for virus replication in cell culture. ProMotif results revealed that the structure of ORF7a protein has 1 sheet, 2 beta hairpins, 3 strands 5 helices, 4 helix-helix interact, 8 beta turns, 1 gamma turn (Figure 3K). ORF7a protein (Molecular Weight = 13743.47 Daltons) is rich in Leucine (12.40%) Threonine (8.26 %) and Phenylalanine (8.26%). ORF7a protein has theoretical Isoelectric point (pI) 8.23, Instability index 48.66, Aliphatic index 100.74 and Grand average of hydropathicity 0.318 (Figure 2H; Table 3).

Protein 7a (SARS coronavirus X4 like protein) (Pfam: PF08779 SARS\_X4) is a unique type I transmembrane protein (Nelson *et al.*, 2005). It has been suggested that it has binding activity to integrin I domains (Hänel *et al.*, 2006). It contains a motif which has been demonstrated to mediate COPII dependent transport out of the endoplasmic reticulum, and the protein is targeted to the Golgi apparatus (InterPro IPR01488) (Pekosz *et al.*, 2006).

## 22. ORF 7b protein

ProMotif results revealed that the structure of ORF7b protein has 2 helices, 1 helix-helix interact, 1 beta turn and 1 gamma turn (Figure 3L). ORF7b protein (Molecular Weight = 5179.98 Daltons) is rich in Leucine (25.58%) and Phenylealanine (13.95%). ORF7b protein has theoretical Isoelectric point (pI) 4.17, Instability index 50.96, Aliphatic index 156.51 and Grand average of hydropathicity 1.449 (Figure 2I; Table 3).

ORF7b has Protein family membership Non-structural protein 7b, SARS-like (IPR021532) (also known as accessory protein 7b, NS7B, ORF7b, and 7b) from human SARS coronavirus (SARS-CoV) and similar betacoronaviruses (Pekosz *et al.*, 2006). It consists of an N-terminal, a C-terminal and a transmembrane domain, the latter is essential to retain the protein in the Golgi compartment (Schaecher *et al.*, 2007, 2008). Despite it being named as "non-structural", it has been reported to be a structural component of SARS-CoV virions and an integral membrane protein (Schaecher *et al.*, 2007).

## 23. ORF8 protein

ProMotif results revealed that the structure of ORF8 protein has 3 sheets, 1 beta bulge, 10 strands, 15 beta turns and 1 gamma turn (Figure 3M). ORF8 protein (Molecular Weight = 13830.33 Daltons) is rich in Valine (9.92%) Leucine (8.26%) and Isoleucine (8.26%). ORF8 protein has theoretical Isoelectric point (pI) 5.42, Instability index 45.79, Aliphatic index 97.36 and Grand average of hydropathicity 0.219 (Figure 2J; Table 3).

ORF8 protein belongs to the family Non-structural protein NS8, betacoronavirus (IPR022722). This family of proteins includes the accessory proteins encoded by the ORF8 in coronaviruses, also known as accessory protein 8, or non-structural protein 8 (NS8). *This is distinct from NSP8, which is encoded on the replicase*

*polyprotein. This protein has two conserved sequence motifs: EDPCP and INCQ. It may modulate viral pathogenicity or replication in favour of human adaptation. ORF8 was suggested as one of the relevant genes in the study of human adaptation of the virus (Keng et al., 2006; Law et al., 2006).*

## 24. Nucleocapsid phosphoprotein

ProMotif results revealed that the structure of Nucleocapsid phosphoprotein has 1 sheet, 1 beta hairpin, 2 strands, 30 helices, 27 helix-helix interacts, 31 beta turns, 11 gamma turns (Figure 3N). Nucleocapsid phosphoprotein (Molecular Weight = 45623.27 Daltons) is rich in Glycine (10.26%), Alanine (8.83%) and Serine (8.83%). Nucleocapsid phosphoprotein has theoretical Isoelectric point (pI) 10.07, Instability index 55.09, Aliphatic index 52.53 and Grand average of hydropathicity -0.971 (Figure 2K; Table 3).

The Nucleocapsid protein family SARS-COV-2 (IPR001218) is the member of protein family Nucleocapsid protein, coronavirus (IPR001218) and Nucleocapsid protein, betacoronavirus (IPR043505). Coronavirus (CoV) nucleocapsid (N) proteins have 3 highly conserved domains. The N-terminal domain (NTD) (N1b), the C-terminal domain (CTD) (N2b) and the N3 region. The N1b and N2b domains from SARS CoV, infectious bronchitis virus (IBV), human CoV 229E and mouse hepatic virus (MHV) display similar topological organisations. N proteins form dimers, which are asymmetrically arranged into octamers via their N2b domains. The protein is cellular component of viral nucleocapsid (GO: 0019013).

Domains N1b and N2b are linked by another domain N2a that contains an SR-rich region (rich in serine and arginine residues). A priming phosphorylation of specific serine residues by an as yet unknown kinase, triggers the subsequent phosphorylation by the host glycogen synthase kinase-3 (GSK-3) of several residues in the SR-rich region. This phosphorylation allows the N protein to associate with the RNA helicase DDX1 permitting template read-through, and enabling the transition from discontinuous transcription of subgenomic mRNAs (sgmRNAs) to continuous synthesis of longer sgmRNAs and genomic RNA (gRNA). Production of gRNA in the presence of N oligomers may promote the formation of ribonucleoprotein complexes, and the newly transcribed sgmRNA would guarantee sufficient synthesis of structural proteins (Wu et al., 2014; Cong et al., 2017, 2020).

It has been shown that N proteins interact with nonstructural protein 3 (NSP3) and thus are recruited to the replication-transcription complexes (RTCs). In MHV, the N1b and N2a domains mediate the binding to NSP3 in a gRNA-independent manner. At the RTCs, the N protein is required for the stimulation of gRNA replication and sgmRNA transcription. It remains unclear, however, how and why the N protein orchestrates viral RNA synthesis. The cytoplasmic N-terminal ubiquitin-like domain of NSP3 and the SR-rich region of the N2a domain of the N protein may be important for this interaction. The direct association of N protein with RTCs is a critical step for MHV infection (Cong et al., 2020). Sequence comparison of the N genes of five strains of the coronavirus mouse hepatitis virus suggests a three domain structure for the nucleocapsid protein (Parker and Masters, 1990).

## 25. ORF10 protein

ProMotif results revealed that the structure of ORF10 protein has 1 sheet, 1 beta alpha beta unit, 2 strands, 1 helix, 2 beta turns (Figure 3O). ORF10 protein (Molecular Weight = 4449.01 Daltons) is rich in Asparagine (13.16%), Leucine (10.53%), and Phenylalanine (10.53%). ORF10 protein has theoretical Isoelectric point (pI) 7.93, Instability index 16.06, Aliphatic index 107.63 and Grand average of hydropathicity 0.637 (Figure 2L; Table 3). Protein family membership has not been predicted for ORF 10 protein.

## Hetero-Oligomeric Complexes

Nsp7-nsp8 hexadecamer may possibly confer processivity to the polymerase, maybe by binding to dsRNA or by producing primers utilized by the latter. Experimental evidence for SARS-CoV that nsp7 and nsp8 activate and confer processivity to the RNA-synthesizing activity of Polymerase (Subissi *et al.*, 2014; Kirchdoerfer and Ward, 2019). Nsp10 plays a pivotal role in viral transcription by stimulating nsp14 3'-5' exoribonuclease activity. Nsp10 plays a pivotal role in viral transcription by stimulating nsp16 2'-O-ribose methyltransferase activity. Spike protein S1 binds to human ACE2, initiating the infection. CoV attaches to the target cells with the help of spike protein–host cell protein interaction (angiotensin converting enzyme-2 [ACE-2] interaction in SARS-CoV (Li *et al.*, 2003) and dipeptidyl peptidase-4 [DPP-4] in MERS-CoV (Mubarak *et al.*, 2019). After the receptor recognition, the virus genome with its nucleocapsid is released into the cytoplasm of the host cells. The viral genome contains ORF1a and ORF1b genes, which produce two PPs that are pp1a and pp1b (te Velthuis *et al.*, 2016) which help to take command over host ribosomes for their own translation process (Stobart *et al.*, 2013).

The Instability index value of SARS-COV-2 ranged between 16.06 (ORF10 protein) and 51.97 (NSP7), which classifies ORF10 protein as most stable and NSP7 as most unstable protein. The proteins namely ORF7a protein (48.66), ORF7b protein (50.96), NSP7 (51.97), ORF 8 protein (45.79) and Nucleocapsid phosphoprotein (55.09) are unstable as per the instability index. The rest of the proteins are showing stability as per the instability index (Table 3). Except Nucleocapsid phosphoprotein and ORF10 protein all other proteins of SARS-COV-2 are rich in Lucine (Figure 2). The aliphatic index of SARS-COV2 ranged between 61.80 (NSP10) and 156.51 (ORF 7b protein), which indicates most thermostability in ORF 7b protein (Table 3). The Grand average of hydropathicity (GRAVY) value of NSP4 (0.343), NSP6 (0.790), NSP7 (0.199), ORF3a protein (0.275), Envelope protein (1.128), Membrane glycoprotein (0.446), ORF6 protein (0.233), ORF7a protein (0.318), ORF 7b protein (1.449), ORF 8 protein (0.219) and ORF10 protein (0.637) indicate that these proteins are hydrophobic in nature. The all other proteins are hydrophilic (Table 3).

The Tunnels, Clefts and pore analysis results for selected proteins of SARS-COV-2, calculated by MOLE 2.0 program version 2.5.13.11.08 and visualized using Pymol 0.97rc has been shown in Figures 4 and 5. The details of predicted structure verification report, Modelarchive structure download link doi (<https://www.modelarchive.org/doi/10.xxxx/>), structural analysis and interpretation for each protein will be provided (in Appendix-I).

## CONCLUSION

The RNA genome of SARS-CoV-2 has 29.9 Kb nucleotides, encoding for 29 proteins, though one may not get expressed. Studying these different components of the virus, as well as how they interact with our cells is already yielding some clues, but much remains to be explored. The present study reported theoretical modeling of 15 proteins, In silico sequence-based and structure-based functional characterization of full SARS-CoV-2 proteome based on the NCBI reference sequence NC\_045512 (29903 bp ss-RNA). The theoretical structures along with statistical verification reports deposited to ModelArchive will be available upon publication of this paper. The 15 theoretical structures will be useful for the scientific community for advanced computational analysis on interactions of each protein for detailed functional analysis of active sites towards structure based drug designing or to study potential vaccines towards preventing epidemics and pandemics in absence of complete experimental structure.



## ACKNOWLEDGEMENTS

The authors are grateful to DBT-Govt. of India for supporting Bioinformatics Laboratory (under DBT-Star College scheme) at Post Graduate Department of Zoology, Darrang College, Tepur, Assam. The authors are thankful to the Principal, Darrang College (Gauhati University), Tezpur (Assam) India and Head of the Post Graduate Department of Zoology, Darrang College for supporting the research laboratory facility.

## REFERENCES

- Altschul, S.F., Madden, T.L., Schaffer, A.A., Zhang, J., Zhang, Z., Miller, W. and Lipman, D.J. 1997. Gapped BLAST and PSI-BLAST: a new generation of protein database search programs. *Nuc. Ac. Res.*, 25(17): 3389-3402.
- Armstrong J, Niemann H, Smeekens S, Rottier P, Warren G. 1984. Sequence and topology of a model intracellular membrane protein, E1 glycoprotein, from a coronavirus. *Nature* 308:751-2, View article PMID: 6325918.
- Campanacci V, Egloff MP, Longhi S, Ferron F, Rancurel C, Salomoni A, Dourousseau C, Tocque F, Bremond N, Dobbe JC, Snijder EJ, Canard B, Cambillau C. 2003. Structural genomics of the SARS coronavirus: cloning, expression, crystallization and preliminary crystallographic study of the Nsp9 protein. *Acta Crystallogr D Biol Crystallogr*; 59:1628-1631.:PUBMED:12925794 EPMC:12925794.
- Chang CK, Jeyachandran S, Hu NJ, Liu CL, Lin SY, Wang YS, et al. 2016. Structure-based virtual screening and experimental validation of the discovery of inhibitors targeted towards the human coronavirus nucleocapsid protein. *Mol Biosyst*;12:59-66.
- Chen Y, Su C, Ke M, Jin X, Xu L, Zhang Z, Wu A, Sun Y, Yang Z, Tien P, Ahola T, Liang Y, Liu X, Guo D. 2011. Biochemical and structural insights into the mechanisms of SARS coronavirus RNA ribose 2'-O-methylation by nsp16/nsp10 protein complex. *PLoS Pathog.* 7:e1002294.: PUBMED:22022266 EPMC:22022266.
- Cheng W, Chen S, Li R, Chen Y, Wang M, Guo D. 2015. Severe acute respiratory syndrome coronavirus protein 6 mediates ubiquitin-dependent proteosomal degradation of N-Myc (and STAT) interactor. *Virology* 530, 153-61; PMID: 25907116.
- Chiu, S.S., Chan, K.H., Chu, K.W., Kwan, S.W., Guan, Y., Poon, L.L., and Peiris, J.S. 2005. Human coronavirus NL63 infection and other coronavirus infections in children hospitalized with acute respiratory disease in Hong Kong, China. *Clin. Infect. Dis.* 40, 1721–1729.
- Cong Y, Kriegenburg F, de Haan CAM, Reggiori F. 2017. Coronavirus nucleocapsid proteins assemble constitutively in high molecular oligomers. *Sci Rep* 7, 5740, PMID: 28720894.
- Cong Y, Ulasli M, Schepers H, Mauthe M, V'kovski P, Kriegenburg F, Thiel V, de Haan CAM, Reggiori F. 2020. Nucleocapsid Protein Recruitment to Replication-Transcription Complexes Plays a Crucial Role in Coronaviral Life Cycle. *J. Virol.* 94, PMID: 31776274.
- Coronaviridae Study Group of the International Committee on Taxonomy of Viruses. 2020. The species Severe acute respiratory syndrome-related coronavirus: classifying 2019-nCoV and naming it SARS-CoV-2. *Nat. Microbiol.* 5, 536–544.
- de Groot, R. J. et al. in *Virus Taxonomy, Ninth Report of the International Committee on Taxonomy of Viruses* (eds King, A. M. Q. et al.) 806–828 (Elsevier Academic Press, 2012).
- Egloff MP, Ferron F, Campanacci V, Longhi S, Rancurel C, Dutartre H, Snijder EJ, Gorbalenya AE, Cambillau C, Canard B. 2004. The severe acute respiratory syndrome-coronavirus replicative protein nsp9 is a single-

- stranded RNA-binding subunit unique in the RNA virus world. , Proc Natl Acad Sci U S A. 101:3792-3796.PUBMED:15007178 EPMC:15007178.
- Eswar, N., Webb, B., Marti-Renom, M.A., Madhusudhan, M.S., Eramian, D., Shen, M.Y., Pieper, U. and Sali, A. 2006. Comparative Protein Structure Modelling Using MODELLER. Ed: Coligan JE, Dunn BM, Speicher DW, Wingfield PT. Current Protocols in Protein Science Unit. 2.9 1-31.
- Finn R.D., Clements J., Eddy S.R. 2011. HMMER Web Server: Interactive Sequence Similarity Searching. R. D. Finn, J. Clements, S. R. Eddy. *Nucleic Acids Research*, 39:W29-37.
- Fiser, A., Do, R.K. and Sali, A. 2000. Modeling of loops in protein structures. *Protein Science*, 9: 1753-1773.
- Gasteiger, E., Hoogland, C., Gattiker, A., Duvaud, S., Wilkins, M.R., Appel, R.D. and Bairoch, A. 2005. Protein Identification and Analysis Tools on the ExPASy Server ;( In) *John M. Walker (ed): The Proteomics Protocols Handbook*, Humana Press pp. 571-607.
- Geng H, Liu YM, Chan WS, Lo AW, Au DM, Waye MM, Ho YY. 2005.The putative protein 6 of the severe acute respiratory syndrome-associated coronavirus: expression and functional characterization. *FEBS Lett.* 579, 6763-8. PMID: 16310783
- Haas J., Gumieny R., Barbato A., Ackermann F., Tauriello G., Bertonni M., Studer G., Smolinski A., Schwede T. 2019, Introducing "best single template" models as reference baseline for the Continuous Automated Model Evaluation (CAMEO). *Proteins*. 87, 1378-1387. [DOI: 10.1002/prot.25815].
- Hänel K, Stangler T, Stoldt M, Willbold D.2006. "Solution structure of the X4 protein coded by the SARS related coronavirus reveals an immunoglobulin like fold and suggests a binding activity to integrin I domains". *J. Biomed. Sci.* 13 (3): 281–93. PMID 16328780. doi:10.1007/s11373-005-9043-9.
- Huang, C. et al. 2020. Clinical features of patients infected with 2019 novel coronavirus in Wuhan, China. *Lancet* 395, 497–506 .
- Jean, A., Quach, C., Yung, A., and Semret, M. 2013. Severity and outcome associated with human coronavirus OC43 infections among children. *Pediatr. Infect. Dis. J.* 32, 325–329.
- Jiang, S., Shi, Z., Shu, Y., Song, J., Gao, G.F., Tan, W., and Guo, D. 2020. A distinct name is needed for the new coronavirus. *Lancet* 395, 949.
- Joseph JS, Saikatendu KS, Subramanian V, Neuman BW, Brooun A, Griffith M, Moy K, Yadav MK, Velasquez J, Buchmeier MJ, Stevens RC, Kuhn P. 2006. Crystal structure of nonstructural protein 10 from the severe acute respiratory syndrome coronavirus reveals a novel fold with two zinc-binding motifs. *J Virol.* 80:7894-7901.: PUBMED:16873246 EPMC:16873246.
- Keng CT, Choi YW, Welkers MR, Chan DZ, Shen S, Gee Lim S, Hong W, Tan. 2006. The human severe acute respiratory syndrome coronavirus (SARS-CoV) 8b protein is distinct from its counterpart in animal SARS-CoV and down-regulates the expression of the envelope protein in infected cells. *YJ. Virology* 354, 132-42, PMID: 16876844.
- Kirchdoerfer, R.N. and Ward, A.B. 2019. Structure of the SARS-CoV nsp12 polymerase bound to nsp7 and nsp8 co-factors. *Nature Communications*, 10(1), pp.1-9.
- Lai, M.M.C., Perlman, S., and Anderson, L.J. 2007. Coronaviridae. In *Fields Virology*, D.M. Knipe and P.M. Howley, eds. (Lippincott Williams & Wilkins), pp. 1305–1335.
- Laskowski, R.A., Watson, J.D. and Thornton, J.M. 2005. ProFunc: a server for predicting protein function from 3D structure. *Nucleic Acids Res.*, 33: W89-W93.
- Law PY, Liu YM, Geng H, Kwan KH, Waye MM, Ho YY. 2006. Expression and functional characterization of the putative protein 8b of the severe acute respiratory syndrome-associated coronavirus. *FEBS Lett.*580, 3643-8, PMID: 16753150

- Li W, Moore MJ, Vasilieva N, Sui J, Wong SK, Berne MA, et al. 2003. Angiotensin-converting enzyme 2 is a functional receptor for the SARS coronavirus. *Nature* 426:450-4.
- Lu W, Zheng BJ, Xu K, Schwarz W, Du L, Wong CK, Chen J, Duan S, Deubel V, Sun B. 2006. Severe acute respiratory syndrome-associated coronavirus 3a protein forms an ion channel and modulates virus release. *Proc. Natl. Acad. Sci. U.S.A.* 103, 12540-5, View article PMID: 16894145
- Lu, G., and Liu, D. 2012. SARS-like virus in the Middle East: a truly bat-related coronavirus causing human diseases. *Protein Cell* 3, 803–805.
- Lu, G., Wang, Q., and Gao, G.F. 2015. Bat-to-human: spike features determining ‘host jump’ of coronaviruses SARS-CoV, MERS-CoV, and beyond. *Trends Microbiol.* 23, 468–478.
- Madan V, Garcia Mde J, Sanz MA, Carrasco L.; 2005. Viroporin activity of murine hepatitis virus E protein. *FEBS Lett.* 579, 3607-12, PMID: 15963987.
- Manolaridis I, Wojdyla JA, Panjekar S, Snijder EJ, Gorbalenya AE, Berglund H, Nordlund P, Coutard B, Tucker PA. 2009. Structure of the C-terminal domain of nsp4 from feline coronavirus. *Acta Crystallogr D Biol Crystallogr.*;65:839-846.: PUBMED:19622868 EPMC:19622868.
- Minakshi R, Padhan K, Rani M, Khan N, Ahmad F, Jameel S. 2009. The SARS Coronavirus 3a protein causes endoplasmic reticulum stress and induces ligand-independent downregulation of the type 1 interferon receptor. *PLoS ONE* 4, e8342, View article PMID:20020050
- Mubarak A, Alturaiki W, Hemida MG. 2019. Middle East Respiratory Syndrome Coronavirus (MERS-CoV): Infection, Immunological Response, and Vaccine Development. *J Immunol Res.*;2019:1-11.
- Nelson CA, Pekosz A, Lee CA, Diamond MS, Fremont DH. 2005. "Structure and intracellular targeting of the SARS-coronavirus Orf7a accessory protein.". *Structure.* 13 (1): 75–85. PMID 15642263. doi:10.1016/j.str.2004.10.010.
- Nieto-Torres JL, Verdia-Baguena C, Jimenez-Guardeno JM, Regla-Nava JA, Castano-Rodriguez C, Fernandez-Delgado R, Torres J, Aguilera VM, Enjuanes L. 2015. Severe acute respiratory syndrome coronavirus E protein transports calcium ions and activates the NLRP3 inflammasome. *Virology* 485, 330-9, PMID:26331680.
- Parker, M. M. & Masters, P. S. 1990. Sequence comparison of the N genes of five strains of the coronavirus mouse hepatitis virus suggests a three domain structure for the nucleocapsid protein. *Virology* 179, 463-468.[CrossRef]
- Paules CI, Marston HD, Fauci AS. Coronavirus infections-More than just the common cold. *JAMA* 2020;323:707.
- Pearson, W.R. 1991. Searching protein sequence libraries: comparison of the sensitivity and selectivity of the Smith-Waterman and FASTA algorithms. *Genomics*, 11(3): 635-50.
- Pearson, W.R. 1991. Searching protein sequence libraries: comparison of the sensitivity and selectivity of the Smith-Waterman and FASTA algorithms. *Genomics*, 11(3): 635-50.
- Pekosz A, Schaecher SR, Diamond MS, Fremont DH, Sims AC, Baric RS.2006. "Structure, expression, and intracellular localization of the SARS-CoV accessory proteins 7a and 7b.". *Adv Exp Med Biol.* 581: 115–20. PMID 17037516. doi:10.1007/978-0-387-33012-9\_20.
- Schaecher SR, Diamond MS, Pekosz A. 2008. The transmembrane domain of the severe acute respiratory syndrome coronavirus ORF7b protein is necessary and sufficient for its retention in the Golgi complex. *J. Virol.* 82, 9477-91. PMID: 18632859
- Schaecher SR, Mackenzie JM, Pekosz A. 2007. The ORF7b protein of severe acute respiratory syndrome coronavirus (SARS-CoV) is expressed in virus-infected cells and incorporated into SARS-CoV particles. *J. Virol.* 81, 718-31, PMID: 17079322

- Schoeman D, Fielding BC. 2019. Coronavirus envelope protein: current knowledge. *Viol. J.* 16, 69, PMID: 31133031.
- Sehnal, D., Svobodová Vařeková, R., Berka, K. *et al.* 2013. MOLE 2.0: advanced approach for analysis of biomacromolecular channels. *J Cheminform* 5, 39 <https://doi.org/10.1186/1758-2946-5-39>.
- Shen S, Lin PS, Chao YC, Zhang A, Yang X, Lim SG, Hong W, Tan YJ. 2005. The severe acute respiratory syndrome coronavirus 3a is a novel structural protein. *Biochem. Biophys. Res. Commun.* 330, 286-92, View article PMID: 15781262
- Siddell, S. G. et al. 2008. Additional changes to taxonomy ratified in a special vote by the International Committee on Taxonomy of Viruses. *Arch. Virol.* 164, 943–946 (2019).
- Stobart CC, Sexton NR, Munjal H, Lu X, Molland KL, Tomar S, et al. 2013. Chimeric exchange of coronavirus nsp5 proteases (3CLpro) identifies common and divergent regulatory determinants of protease activity. *J Virol.* 87:12611-8.
- Subissi, L., Posthuma, C.C., Collet, A., Zevenhoven-Dobbe, J.C., Gorbalenya, A.E., Decroly, E., Snijder, E.J., Canard, B. and Imbert, I., 2014. One severe acute respiratory syndrome coronavirus protein complex integrates processive RNA polymerase and exonuclease activities. *Proceedings of the National Academy of Sciences*, 111(37), pp.E3900-E3909.
- Surya W, Li Y, Verdia-Baguena C, Aguilera VM, Torres. 2015. MERS coronavirus envelope protein has a single transmembrane domain that forms pentameric ion channels. *J. Virus Res.* 201, 61-66. View article PMID: 25733052.
- te Velthuis AJ, van den Worm SH, Snijder EJ. 2012. The SARS-coronavirus nsp7+nsp8 complex is a unique multimeric RNA polymerase capable of both de novo initiation and primer extension. *Nucleic Acids Res* 40:1737-47.
- Ujike M, Taguchi F. 2015. Incorporation of spike and membrane glycoproteins into coronavirus virions. *Viruses* 7, 1700-25, PMID: 25855243.
- Webb B., Sali A.. 2016. Comparative Protein Structure Modeling Using Modeller. *Current Protocols in Bioinformatics* 54, John Wiley & Sons, Inc., 5.6.1-5.6.37.
- Woo PC, Lau SK, Lam CS, et al. 2012. Discovery of seven novel Mammalian and avian coronaviruses in the genus deltacoronavirus supports bat coronaviruses as the gene source of alphacoronavirus and betacoronavirus and avian coronaviruses as the gene source of gammacoronavirus and deltacoronavirus. *J Virol.*;86(7):3995–4008. doi:10.1128/JVI.06540-11
- Wu CH, Chen PJ, Yeh SH. 2014. Nucleocapsid phosphorylation and RNA helicase DDX1 recruitment enables coronavirus transition from discontinuous to continuous transcription. *Cell Host Microbe* 16, 462-72,. PMID: 25299332
- Wu, F., Zhao, S., Yu, B., Chen, Y.-M., Wang, W., Song, Z.-G., Hu, Y., Tao, Z.-W., Tian, J.-H., Pei, Y.-Y., et al. 2020. A new coronavirus associated with human respiratory disease in China. *Nature* 579, 265–269.
- Yang H, Bartlam M, Rao Z. Drug design targeting the main protease, the Achilles' heel of coronaviruses. *Curr Pharm Des* 2006;12:4573-90.
- Yu CJ, Chen YC, Hsiao CH, Kuo TC, Chang SC, Lu CY, Wei WC, Lee CH, Huang LM, Chang MF, Ho HN, Lee FJ. 2004. Identification of a novel protein 3a from severe acute respiratory syndrome coronavirus. *FEBS Lett.* 565:111-116. PUBMED:15135062 EPMC:15135062.
- Zhai Y, Sun F, Li X, Pang H, Xu X, Bartlam M, Rao Z. 2005. Insights into SARS-CoV transcription and replication from the structure of the nsp7-nsp8 hexadecamer. *Nat Struct Mol Biol.* 12:980-986.: PUBMED:16228002 EPMC:16228002.

- Zhou, P., Yang, X.-L., Wang, X.-G., Hu, B., Zhang, L., Zhang, W., Si, H.-R., Zhu, Y., Li, B., Huang, C.-L., et al. (2020). A pneumonia outbreak associated with a new coronavirus of probable bat origin. *Nature* 579, 270–273.
- Zhu, N., Zhang, D., Wang, W., Li, X., Yang, B., Song, J., Zhao, X., Huang, B., Shi, W., Lu, R., et al. 2020. A novel coronavirus from patients with pneumonia in China, 2019. *N. Engl. J. Med.* 382, 727–733.
- Ziebuhr, J. *et al.* Proposal 2017.013S. A.v1. Reorganization of the family Coronaviridae into two families, Coronaviridae (including the current subfamily Coronavirinae and the new subfamily Letovirinae) and the new family Tobaniviridae (accommodating the current subfamily Torovirinae and three other subfamilies), revision of the genus rank structure and introduction of a new subgenus rank. (ICTV, 2017); <https://ictv.global/proposal/2017.Nidovirales/>.
- Ziebuhr, J. *et al.* Proposal 2019.021S.Ac.v1. Create ten new species and a new genus in the subfamily Orthocoronavirinae of the family Coronaviridae and five new species and a new genus in the subfamily Serpentovirinae of the family.

**Table 1. Complete Proteome of Severe acute respiratory syndrome coronavirus 2 (SARS-CoV-2) (Genome: NCBI LOCUS NC\_045512; 29903 bp ss-RNA)**

Genome Location	GENE NAME	PRODUCT	NCBI PROTEIN ID
266..21555	ORF1ab	ORF1ab polyprotein	YP_009724389.1
266..13483	ORF1ab	orf1a polyprotein	YP_009725295.1
266..805	ORF1ab	Leather protein (nsp1)	YP_009725297.1
806..2719	ORF1ab	nsp2	YP_009725298.1
2720..8554	ORF1ab	nsp3	YP_009725299.1
8555..10054	ORF1ab	nsp4	YP_009725300.1
10055..10972	ORF1ab	3C-like proteinase	YP_009725301.1
10973..11842	ORF1ab	nsp6	YP_009725302.1
11843..12091	ORF1ab	nsp7	YP_009725303.1
12092..12685	ORF1ab	nsp8	YP_009725304.1
12686..13024	ORF1ab	nsp9	YP_009725305.1
13025..13441	ORF1ab	nsp10	YP_009725306.1
Join(13442..13468,13468..16236)	ORF1ab	RNA-dependent polymerase	YP_009725307.1
16237..18039	ORF1ab	Helicase	YP_009725308.1
18040..19620	ORF1ab	3'-to-5' exonuclease	YP_009725309.1
19621..20658	ORF1ab	EndoRNase	YP_009725310.1
20659..21552	ORF1ab	2'-O-ribose methyltransferase	YP_009725311.1
21563..25384	S	structural protein; spike protein	YP_009724390.1
25393..26220	ORF3a	ORF3a protein	YP_009724391.1
26245..26472	E	envelope protein	YP_009724392.1
26523..27191	M	membrane glycoprotein	YP_009724393.1
27202..27387	ORF6	ORF6 protein	YP_009724394.1
27394..27759	ORF7a	ORF7a protein	YP_009724395.1
27756..27887	ORF7b	ORF7b	YP_009725318.1
27894..28259	ORF8	ORF8 protein	YP_009724396.1
28274..29533	N	Nucleocapsid phosphoprotein	YP_009724397.2
29558..29674	ORF10	ORF10 protein	YP_009725255.1

**Table 2.** BLAST results against available PDB structures for selection of modeling method, template selection and existing PDB structures considered.

Sl no.	Protein name and NCBI Accession number	LENGTH (aa residue)	PDB TEMPLATE (S)	Identity with template (%)	E-value	Query coverage	The final structure/modeling method selected
1	<b>Leader protein</b> (NSP1) (YP_009725297.1)	180	2GDT_A	86.09%	6e-67	63%	**Comparative modelling
2	<b>NSP2</b> (YP_009725298.1)	638	1JWH_C	32.56%	5.9	6%	<i>Ab-initio</i> modelling
3	<b>NSP3</b> (YP_009725299.1)	1945	2W2G_A	75.00%	13%	3e-133	<i>Ab-initio</i> modelling
			6W9C_A	100.00%	0.0	16%	
4	<b>NSP4</b> (YP_009725300.1)	500	3VCB_A	59.78%	3e-29	18%	<i>Ab-initio</i> modelling
5	<b>3C-like proteinase</b> (YP_009725301.1)	306	5R7Y_A	100.00%	0.0	100%	5R7Y_A*
6	<b>NSP6</b> (YP_009725302.1)	290	6GW5_A	29.17%	2.6	24%	Comparative modelling
			3PLS_A	24.29%	7.6	24%	
7	<b>NSP7</b> (YP_009725303.1)	83	7BV1_C	100.00%	1e-54	100.00%	7BV1_C*
8	<b>NSP8</b> (YP_009725304.1)	198	7BV1_B	100.00%	3e-147	100.00%	7BV1_B*
9	<b>NSP9</b> (YP_009725305.1)	113	6W9Q_A	100.00%	5e-82	100.00%	6W9Q_A*
10	<b>NSP10</b> (YP_009725306.1)	139	6W4H_B	100.00%	8e-103	100.00%	6W4H_B*
11	<b>RNA-dependent polymerase</b> (YP_009725307.1)	932	6M71_A	100.00%	0.0	100.00%	6M71_A*
12	<b>Helicase</b> (YP_009725308.1)	601	6JYT_A	98.50%	0.0	100%	6JYT_A*
13	<b>3'-to-5' exonuclease</b> (YP_009725309.1)	527	5C8S_B	95.07%	0.0	100%	5C8S_B*
14	<b>endoRNase/ NSP15</b> (YP_009725310.1)	346	6WLC_A	100.00%	0.0	100.00%	6WLC_A*
15	<b>2'-O-ribose methyltransferase</b> (YP_009725311.1)	298	6W4H_A	100.00%	0.0	100.00%	6W4H_A*
16	<b>Surface glycoprotein/ spike glycoprotein</b> (QJF77858.1)	1273	6VSB_A	99.50%	0.0	94%	**Comparative modelling
17	<b>ORF3a protein</b> (QJF77859.1")	275	No hits	-	-	-	<i>Ab-initio</i> modelling
18	<b>Envelope protein</b> (QJF77860.1)	75	5X29_A	88.71%	1e-30	-	Comparative modelling
19	<b>Membrane glycoprotein</b> (QJF77861.1)	222	3OIS_A	27.45%	9.0	22%	<i>Ab-initio</i> modelling
20	<b>ORF6 protein</b> (QJF77862.1)	61	No hits	-	-	-	<i>Ab-initio</i> modelling
21	<b>ORF7a protein</b> (QJF77863.1)	121	6W37_A	100.00%	1e-46	55%	Comparative modelling
22	<b>ORF7b</b> (QJF77864.1)	43	No hits	-	-	-	<i>Ab-initio</i> modelling
23	<b>ORF8 protein</b> (QJF77865.1)	121	5O32_I	25.00%	5.7	47%	Comparative modelling
24	<b>Nucleocapsid phosphoprotein</b> (QJF77866.1)	419	6WJI_A	100.00%	2e-82	28%	Comparative modelling
			6YI3_A	99.28%	3e-98	32%	
25	<b>ORF10 protein</b> (QJF77867.1)	38	Not hits	-	-	-	<i>Ab-initio</i> modelling

\* Have experimental structures with PDB ID, no modeling required.

\*\*Have experimental structures low query coverage, modeling required.



**Table 3.** Physicochemical parameters of SARS-CoV-2 proteome

PROTEIN NAME	MW (Da)	pI	formula	Ext. coefficient Abs 0.1% (=1 g/l)	Instability index	Aliphatic index	GRAVY*
ORF1ab polyprotein (YP_009724389.1)	794057.79	6.32	C <sub>35644</sub> H <sub>55333</sub> N <sub>9253</sub> O <sub>10496</sub> S <sub>394</sub>	942275	33.31	86.87	-0.070
ORF1a polyprotein (YP_009725295.)	489988.91	6.04	C <sub>21982</sub> H <sub>34326</sub> N <sub>5654</sub> O <sub>6524</sub> S <sub>243</sub>	552175	34.92	88.99	-0.023
NSP1 (YP_009725297.1)	19775.31	5.36	C <sub>872</sub> H <sub>1383</sub> N <sub>247</sub> O <sub>270</sub> S <sub>4</sub>	12950	28.83	89.72	-0.378
NSP2 (YP_009725298.1)	70511.38	6.25	C <sub>3149</sub> H <sub>4986</sub> N <sub>820</sub> O <sub>937</sub> S <sub>37</sub>	68435	36.06	88.93	-0.062
NSP3 (YP_009725299.1)	217252.61	5.56	C <sub>9722</sub> H <sub>15175</sub> N <sub>2489</sub> O <sub>2969</sub> S <sub>88</sub>	243675	36.56	86.22	-0.175
NSP4 (YP_009725300.1)	56183.98	7.16	C <sub>2592</sub> H <sub>3925</sub> N <sub>631</sub> O <sub>716</sub> S <sub>25</sub>	81680	34.09	95.50	0.343
3C-like proteinase (YP_009725301.1)	33796.64	5.95	C <sub>1499</sub> H <sub>2318</sub> N <sub>402</sub> O <sub>445</sub> S <sub>22</sub>	33640	27.65	82.12	-0.019
NSP6 (YP_009725302.1)	33033.69	9.11	C <sub>1546</sub> H <sub>2378</sub> N <sub>360</sub> O <sub>385</sub> S <sub>27</sub>	58955	22.94	111.55	0.790
NSP7 (YP_009725303.1)	9239.82	5.18	C <sub>400</sub> H <sub>675</sub> N <sub>107</sub> O <sub>127</sub> S <sub>7</sub>	5625	51.97	117.35	0.199
NSP8 (YP_009725304.1)	21881.08	6.58	C <sub>958</sub> H <sub>1552</sub> N <sub>260</sub> O <sub>301</sub> S <sub>11</sub>	20065	37.78	88.33	-0.192
NSP9 (YP_009725305.1)	12378.20	9.10	C <sub>549</sub> H <sub>876</sub> N <sub>150</sub> O <sub>165</sub> S <sub>5</sub>	13075	34.17	82.92	-0.227
NSP10 (YP_009725306.1)	14789.92	6.29	C <sub>636</sub> H <sub>991</sub> N <sub>173</sub> O <sub>199</sub> S <sub>17</sub>	13700	34.56	61.80	-0.068
RNA-dependent RNA polymerase (YP_009725307.1)	106660.24	6.14	C <sub>4792</sub> H <sub>7265</sub> N <sub>1259</sub> O <sub>1401</sub> S <sub>54</sub>	137670	28.32	78.43	-0.224
Helicase (YP_009725308.1)	66854.75	8.66	C <sub>2981</sub> H <sub>4670</sub> N <sub>800</sub> O <sub>878</sub> S <sub>34</sub>	68785	33.31	84.49	-0.096
3'-to-5' exonuclease (YP_009725309.1)	59815.67	7.80	C <sub>2696</sub> H <sub>4093</sub> N <sub>717</sub> O <sub>757</sub> S <sub>36</sub>	93625	28.85	78.96	-0.134
endoRNase/ NSP15 (YP_009725310.1)	38813.40	5.06	C <sub>1759</sub> H <sub>2743</sub> N <sub>445</sub> O <sub>523</sub> S <sub>10</sub>	33140	36.28	95.09	-0.076
2'-O-ribose methyltransferase (YP_009725311.1)	33323.32	7.59	C <sub>1493</sub> H <sub>2331</sub> N <sub>393</sub> O <sub>437</sub> S <sub>17</sub>	56630	26.11	90.64	-0.086
Surface glycoprotein (QJF77858.1)	141120.43	6.32	C <sub>6334</sub> H <sub>9768</sub> N <sub>1656</sub> O <sub>1892</sub> S <sub>54</sub>	148960	32.86	84.67	-0.077
ORF3a protein (QJF77859.1)	31122.94	5.55	C <sub>1440</sub> H <sub>2189</sub> N <sub>343</sub> O <sub>404</sub> S <sub>11</sub>	58705	32.96	103.42	0.275
Envelope protein (QJF77860.1)	8365.04	8.57	C <sub>390</sub> H <sub>625</sub> N <sub>91</sub> O <sub>103</sub> S <sub>4</sub>	6085	38.68	144.00	1.128
Membrane glycoprotein (QJF77861.1)	25146.62	9.51	C <sub>1165</sub> H <sub>1823</sub> N <sub>303</sub> O <sub>301</sub> S <sub>8</sub>	52160	39.14	120.86	0.446
ORF6 protein (QJF77862.1)	7272.54	4.60	C <sub>334</sub> H <sub>532</sub> N <sub>78</sub> O <sub>96</sub> S <sub>3</sub>	8480	31.16	130.98	0.233
ORF7a protein (QJF77863.1)	13744.17	8.23	C <sub>633</sub> H <sub>988</sub> N <sub>156</sub> O <sub>171</sub> S <sub>7</sub>	7825	48.66	100.74	0.318
ORF7b protein (QJF77864.1)	5180.27	4.17	C <sub>251</sub> H <sub>374</sub> N <sub>50</sub> O <sub>60</sub> S <sub>4</sub>	7115	50.96	156.51	1.449
ORF8 protein (QJF77865.1)	13831.01	5.42	C <sub>633</sub> H <sub>961</sub> N <sub>155</sub> O <sub>177</sub> S <sub>8</sub>	16305	45.79	97.36	0.219

Nucleocapsid phosphoprotein (QJF77866.1)	45625.70	10.07	C <sub>1971</sub> H <sub>3137</sub> N <sub>607</sub> O <sub>629</sub> S <sub>7</sub>	43890	55.09	52.53	-0.971
ORF10 protein (QJF77867.1)	4449.23	7.93	C <sub>206</sub> H <sub>312</sub> N <sub>50</sub> O <sub>54</sub> S <sub>3</sub>	4470	16.06	107.63	0.637

\*GRAVY: Grand average of hydropathicity

**Table 4.** Predicted functions of SARS-CoV-2 proteome with respective ProFunc score (shown within parenthesis)

PROTEIN NAME	Summary of predicted function			
	Protein name terms	Gene Ontology (GO) terms		
		Cellular component	Biological process	Biochemical function
NSP1 (YP_009725297.1)	<b>bound</b> (1.75) <b>human</b> (1.00) <b>streptococcus</b> (1.00) <b>nucleoside</b> (0.77) <b>nmr</b> (0.70) <b>nonstructural</b> (0.70) <b>nsp1</b> (0.70) <b>sars coronavirus</b> (0.70)	<b>cytoplasm</b> (0.50) <b>cytosol</b> (0.50) <b>cell</b> (0.50) <b>cell part</b> (0.50)	<b>metabolic process</b> (1.75) <b>catabolic process</b> (1.26) <b>primary metabolic process</b> (1.26) <b>cellular process</b> (1.00)	<b>catalytic activity</b> (2.21) <b>binding</b> (1.26) <b>transferase activity</b> (1.25) <b>metal ion binding</b> (0.89)
NSP2 (YP_009725298.1)	<b>domain</b> (1.06) <b>dehydrogenase</b> (1.00) <b>binding</b> (0.89) <b>variant</b> (0.88) <b>bound</b> (0.84) <b>zp-c domain</b> (0.56) <b>bmrr</b> (0.55) <b>myelin</b> (0.54)	<b>cytoplasm</b> (2.57) <b>cell</b> (2.57) <b>cell part</b> (2.57) <b>intracellular</b> (2.57)	<b>metabolic process</b> (3.52) <b>primary metabolic process</b> (2.40) <b>cellular process</b> (1.69) <b>cellular metabolic process</b> (1.69)	<b>binding</b> (4.05) <b>catalytic activity</b> (3.12) <b>metal ion binding</b> (2.06) <b>ion binding</b> (2.06)
NSP3 (YP_009725299.1)	<b>ubiquitin</b> (3.09) <b>papain-like protease</b> (2.16) <b>domain</b> (1.95) <b>sars-cov</b> (1.32) <b>enzyme</b> (1.20) <b>coronavirus</b> (1.19) <b>virus</b> (1.10) <b>ubiquitin carboxyl-terminal hydrolase</b> (1.05)	<b>lysosome</b> (0.70) <b>cytosol</b> (0.70) <b>cell</b> (0.70) <b>cell part</b> (0.70)	<b>metabolic process</b> (1.22) <b>proteolysis</b> (0.99) <b>catabolic process</b> (0.99) <b>macromolecule catabolic process</b> (0.99)	<b>metal ion binding</b> (0.83) <b>binding</b> (0.83) <b>ion binding</b> (0.83) <b>cation binding</b> (0.83)
NSP4 (YP_009725300.1)	<b>pneumoniae</b> (1.06) <b>domain</b> (0.86) <b>chemokine receptor</b> (0.83) <b>penicillin-binding</b> (0.55) <b>pbp-2b</b> (0.55) <b>streptococcus pneumoniae</b> (0.55) <b>cytochrome</b> (0.50) <b>ba3</b> (0.50)	<b>cell</b> (3.46) <b>cell part</b> (3.46) <b>membrane</b> (2.21) <b>membrane part</b> (2.21)	<b>metabolic process</b> (4.66) <b>cellular process</b> (4.25) <b>cellular metabolic process</b> (3.86) <b>primary metabolic process</b> (2.76)	<b>binding</b> (3.91) <b>catalytic activity</b> (2.74) <b>metal ion binding</b> (2.56) <b>ion binding</b> (2.56)
3C-like proteinase (YP_009725301.1)	<b>protease</b> (9.00) <b>main</b> (3.26) <b>domain</b> (2.90) <b>main protease</b> (2.72) <b>coronavirus</b> (1.84) <b>virus</b> (1.80) <b>proteinase</b> (1.57) <b>staphylococcus aureus</b> (1.51)	<b>plasma membrane</b> (0.97) <b>membrane</b> (0.97) <b>integral to membrane</b> (0.97) <b>outer membrane-bounded periplasmic space</b> (0.97)	<b>proteolysis</b> (3.16) <b>metabolic process</b> (3.16) <b>catabolic process</b> (3.16) <b>macromolecule catabolic process</b> (3.16)	<b>peptidase activity</b> (3.16) <b>serine \-type peptidase activity</b> (3.16) <b>hydrolase activity</b> (3.16) <b>catalytic activity</b> (3.16)
NSP6 (YP_009725302.1)	<b>domain</b> (1.76) <b>human</b> (1.47) <b>n-terminal domain</b> (0.83) <b>human class</b> (0.77) <b>metabotropic glutamate receptor</b> (0.77)	<b>cell</b> (3.97) <b>cell part</b> (3.97) <b>intracellular</b> (2.36) <b>intracellular part</b> (2.36)	<b>cellular process</b> (2.88) <b>metabolic process</b> (2.86) <b>primary metabolic process</b> (2.17) <b>cellular metabolic</b>	<b>binding</b> (3.71) <b>catalytic activity</b> (3.02) <b>protein binding</b> (2.21) <b>hydrolase activity</b> (1.85)
NSP7	<b>virus</b> (2.35) <b>polymerase</b> (2.21)		<b>glutamate catabolic</b>	<b>binding</b> (0.78) <b>catal</b>

(YP_009725303.1)	<b>rna</b> (1.88) <b>virus rna</b> (1.20) <b>rna polymerase</b> (1.17) <b>rna-dependent rna polymerase</b> (1.00) <b>human</b> (0.99) <b>sars-cov super</b> (0.90)	<b>virion</b> (0.50)	<b>process via L\citramalate</b> (0.50) <b>an aerobic glutamate catabolic process</b> (0.50) <b>cellular process</b> (0.50) <b>cellular metabolic process</b> (0.50)	<b>ytic activity</b> (0.78) <b>protein binding</b> (0.50) <b>isomerase activity</b> (0.50)
NSP8 (YP_009725304.1)	<b>virus</b> (2.35) <b>polymerase</b> (2.21) <b>rna</b> (1.88) <b>virus rna</b> (1.20) <b>rna polymerase</b> (1.17) <b>rna-dependent rna polymerase</b> (1.00) <b>human</b> (0.99) <b>sars-cov super</b> (0.90)	<b>virion</b> (0.50)	<b>glutamate catabolic process via L\citramalate</b> (0.50) <b>an aerobic glutamate catabolic process</b> (0.50) <b>cellular process</b> (0.50) <b>cellular metabolic process</b> (0.50)	<b>binding</b> (0.78) <b>catalytic activity</b> (0.78) <b>protein binding</b> (0.50) <b>isomerase activity</b> (0.50)
NSP9 (YP_009725305.1)	<b>nsp9</b> (1.60) <b>domain</b> (1.20) <b>coronavirus</b> (1.10) <b>sars-coronavirus nsp9</b> (0.90) <b>sars-coronavirus nsp9 g104e</b> (0.90) <b>receptor</b> (0.81) <b>bound</b> (0.81)	<b>cytoplasm</b> (1.33) <b>cell part</b> (1.33) <b>intracellular</b> (1.33)	<b>metabolic process</b> (1.70) <b>catabolic process</b> (1.70) <b>primary metabolic process</b> (1.70) <b>cellular process</b> (1.34)	<b>hydrolase activity</b> (1.76) <b>catalytic activity</b> (1.76) <b>hydrolase activity\, acting on ester bonds</b> (1.30) <b>binding</b> (1.22)
NSP10 (YP_009725306.1)	<b>sars coronavirus</b> (2.11) <b>methyltransferase</b> (2.01) <b>nsp10</b> (1.80) <b>dehydrogenase</b> (1.39) <b>nsp16</b> <b>nsp10</b> <b>sars coronavirus</b> (0.90) <b>nsp10/nsp16</b> (0.90) <b>reovirus core</b> (0.90) <b>chikungunya virus nsp2</b> <b>protease</b> (0.90)	<b>cell</b> (1.01) <b>cell part</b> (1.01) <b>intracellular</b> (1.01) <b>intracellular part</b> (1.01)	<b>metabolic process</b> (4.63) <b>cellular process</b> (3.74) <b>cellular metabolic process</b> (3.74) <b>methylation</b> (2.48)	<b>catalytic activity</b> (4.63) <b>binding</b> (3.73) <b>methyltransferase activity</b> (2.48) <b>transferase activity</b> (2.48)
RNA-dependent RNA polymerase (YP_009725307.1)	<b>human</b> (1.64) <b>domain</b> (1.00) <b>phospholipase</b> (1.00) <b>aps kinase</b> (0.52) <b>penicillium chrysogenum</b> <b>ternary</b> (0.52) <b>adp</b> (0.52) <b>repeats</b> (0.50) <b>chicken brain alpha spectrin</b> (0.50)	<b>cell</b> (1.70) <b>cell part</b> (1.70) <b>intracellular</b> (1.70) <b>intracellular part</b> (1.70)	<b>cellular process</b> (2.20) <b>metabolic process</b> (2.13) <b>cellular metabolic process</b> (1.70) <b>primary metabolic process</b> (1.70)	<b>catalytic activity</b> (2.63) <b>binding</b> (2.62) <b>metal ion binding</b> (1.41) <b>ion binding</b> (1.41)
Helicase (YP_009725308.1)	<b>helicase</b> (5.47) <b>human</b> (1.89) <b>mitochondrial</b> (1.38) <b>fl- atpase</b> (1.26)	<b>cell</b> (4.53) <b>cell part</b> (4.53) <b>intracellular</b> (4.53) <b>intracellular part</b> (4.53)	<b>cellular process</b> (5.07) <b>cellular metabolic process</b> (4.53) <b>nucleobase\, nucleoside\, nucleotide and nucleic acid metabolic process</b> (4.53) <b>metabolic process</b> (4.53)	<b>nucleotide binding</b> (5.07) <b>ATP binding</b> (5.07)
3'-to-5' exonuclease (YP_009725309.1)	<b>dna</b> (3.37) <b>polymerase</b> (3.37) <b>dna polymerase</b> (2.69) <b>exonuclease</b> (1.78) <b>rnase</b> (1.70) <b>type dna polymerase</b> (1.40) <b>angstrom</b> (1.40) <b>coli</b> (1.29)	<b>cytoplasm</b> (3.00) <b>cell part</b> (3.00) <b>intracellular</b> (3.00)	<b>cellular process</b> (7.14) <b>cellular metabolic process</b> (7.14) <b>cellular macromolecule metabolic process</b> (7.14) <b>metabolic process</b> (7.14)	<b>catalytic activity</b> (7.14) <b>binding</b> (6.43) <b>nuclease activity</b> (6.32) <b>hydrolase activity</b> (6.32)

endoRNase/ NSP15 (YP_00972531 0.1)	<b>bound</b> (0.97) <b>sars</b> (0.90) <b>mutati</b> <b>on mhv coronavirus non-</b> <b>structural</b> (0.90) <b>nsp15</b> <b>f307l</b> (0.90) <b>xendou splicing</b> <b>independent</b> <b>snorna</b> (0.90) <b>splicing</b> <b>independent snorna</b> <b>processing</b> (0.90) <b>independent</b> <b>snorna processing</b> <b>endoribonuclease</b> (0.90)	<b>cell</b> (3.16) <b>cell</b> <b>part</b> (3.16) <b>intracellul</b> <b>ar</b> (2.86) <b>intracellular</b> <b>part</b> (2.86)	<b>cellular</b> <b>process</b> (3.17) <b>cellula</b> <b>r metabolic</b> <b>process</b> (2.85) <b>metabo</b> <b>lic</b> <b>process</b> (2.85) <b>primar</b> <b>y metabolic</b> <b>process</b> (2.44)	<b>binding</b> (3.44) <b>cataly</b> <b>tic</b> <b>activity</b> (2.40) <b>metal</b> <b>ion</b> <b>binding</b> (2.24) <b>ion</b> <b>binding</b> (2.24)
2'-O-ribose methyltransfera se (YP_00972531 1.1)	<b>sars</b> <b>coronavirus</b> (2.11) <b>methyltrans</b> <b>ferase</b> (2.01) <b>nsp10</b> (1.80) <b>dehy</b> <b>drogenase</b> (1.39) <b>nsp16 nsp10</b> <b>sars</b> <b>coronavirus</b> (0.90) <b>nsp10/nsp1</b> <b>6</b> (0.90) <b>reovirus</b> <b>core</b> (0.90) <b>chikungunya virus</b> <b>nsp2 protease</b> (0.90)	<b>cell</b> (1.01) <b>cell</b> <b>part</b> (1.01) <b>intracellul</b> <b>ar</b> (1.01) <b>intracellular</b> <b>part</b> (1.01)	<b>metabolic</b> <b>process</b> (4.63) <b>cellula</b> <b>r</b> <b>process</b> (3.74) <b>cellula</b> <b>r metabolic</b> <b>process</b> (3.74) <b>methyl</b> <b>ation</b> (2.48)	<b>catalytic</b> <b>activity</b> (4.63) <b>bindin</b> <b>g</b> (3.73) <b>methyltrans</b> <b>ferase</b> <b>activity</b> (2.48) <b>transf</b> <b>erase activity</b> (2.48)
Surface glycoprotein (QJF77858.1)	<b>coronavirus</b> (4.75) <b>domain</b> (4.3 3) <b>spike</b> (3.39) <b>receptor</b> (3.27) <b>r</b> <b>eceptor-binding</b> <b>domain</b> (2.59) <b>sars</b> (2.58) <b>huma</b> <b>n</b> (1.85) <b>sars coronavirus</b> (1.71)	<b>cytoplasm</b> (0.50) <b>cell</b> ( 0.50) <b>cell</b> <b>part</b> (0.50) <b>intracellul</b> <b>ar</b> (0.50)	<b>glycine biosynthetic</b> <b>process</b> (0.50) <b>one/-</b> <b>carbon compound</b> <b>metabolic</b> <b>process</b> (0.50) <b>cellula</b> <b>r amino acid</b> <b>biosynthetic</b> <b>process</b> (0.50) <b>glycine</b> <b>biosynthetic process</b> <b>from serine</b> (0.50)	<b>glycine</b> <b>hydroxymethyltrans</b> <b>ferase</b> <b>activity</b> (0.50) <b>methy</b> <b>ltransferase</b> <b>activity</b> (0.50) <b>transf</b> <b>erase</b> <b>activity</b> (0.50) <b>pyrid</b> <b>oxal phosphate</b> <b>binding</b> (0.50)
ORF3a protein (QJF77859.1)	<b>dna</b> (1.78) <b>dna</b> <b>glycosylase</b> (1.01) <b>mycobacteri</b> <b>um</b> <b>tuberculosis</b> (0.87) <b>bound</b> (0.87 ) <b>onconase double</b> (0.52) <b>p2y12</b> <b>receptor</b> (0.50) <b>2mesadp</b> (0.50) <b>spontaneously- assembled amp</b> <b>stack</b> (0.50)	<b>cell</b> (1.81) <b>cell</b> <b>part</b> (1.81) <b>cytoplasm</b> (0.88) <b>intracellular</b> ( 0.88)	<b>metabolic</b> <b>process</b> (2.99) <b>cellula</b> <b>r</b> <b>process</b> (2.48) <b>cellula</b> <b>r metabolic</b> <b>process</b> (2.48) <b>primar</b> <b>y metabolic</b> <b>process</b> (2.07)	<b>binding</b> (3.04) <b>cataly</b> <b>tic</b> <b>activity</b> (2.76) <b>metal</b> <b>ion</b> <b>binding</b> (2.30) <b>ion</b> <b>binding</b> (2.30)
Envelope protein (QJF77860.1)	<b>domain</b> (0.91) <b>human</b> (0.53) <b>cc</b> <b>a-adding</b> <b>enzyme</b> (0.53) <b>pyruvate</b> <b>carboxylase</b> (0.50) <b>rhizobium</b> <b>etli</b> (0.50) <b>golgi complex-</b> <b>targeting signal</b> <b>coronavirus</b> (0.50) <b>complex-</b> <b>targeting signal coronavirus</b> <b>envelope</b> (0.50) <b>full-length</b> <b>human mitochondrial cca-</b> <b>adding</b> (0.50)	<b>intracellular</b> (0.95) <b>c</b> <b>ell</b> (0.95) <b>cell</b> <b>part</b> (0.95) <b>intracellul</b> <b>ar part</b> (0.95)	<b>metabolic</b> <b>process</b> (0.95) <b>tRNA</b> <b>3'-terminal CCA</b> <b>addition</b> (0.53) <b>tRNA</b> <b>processing</b> (0.53) <b>tRN</b> <b>A 3'-end</b> <b>processing</b> (0.53)	<b>binding</b> (1.42) <b>cataly</b> <b>tic</b> <b>activity</b> (1.42) <b>nucleo</b> <b>tide</b> <b>binding</b> (1.05) <b>ATP</b> <b>binding</b> (1.05)
Membrane glycoprotein (QJF77861.1)	<b>peptide</b> (1.35) <b>coli</b> (1.35) <b>transp</b> <b>orter</b> (1.27) <b>domain</b> (0.80) <b>xylel</b> <b>la</b> <b>fastidiosa</b> (0.79) <b>oppa</b> (0.61) <b>vir</b> <b>al</b> (0.51) <b>rna polymerase</b> (0.51)	<b>cell</b> (3.76) <b>cell</b> <b>part</b> (3.76) <b>membran</b> <b>e</b> (2.06) <b>integral to</b> <b>membrane</b> (1.67)	<b>establishment of</b> <b>localization</b> (2.10) <b>tra</b> <b>nsport</b> (2.10) <b>localizat</b> <b>ion</b> (2.10) <b>metabolic</b> <b>process</b> (2.01)	<b>binding</b> (3.58) <b>cataly</b> <b>tic</b> <b>activity</b> (2.79) <b>protei</b> <b>n</b> <b>binding</b> (2.43) <b>nucle</b> <b>otide binding</b> (2.08)
ORF6 protein (QJF77862.1)	<b>domain</b> (1.74) <b>human</b> (1.36) <b>bi</b> <b>nding</b> (1.21) <b>binding</b> <b>domain</b> (1.00) <b>bound</b> (1.00) <b>syn</b> <b>thase</b> (0.89) <b>nmr</b> (0.82) <b>region</b> ( 0.82)	<b>cell</b> (2.02) <b>cell</b> <b>part</b> (2.02) <b>cytoplasm</b> (1.64) <b>intracellular</b> ( 1.64)	<b>cellular</b> <b>process</b> (2.15) <b>cellula</b> <b>r metabolic</b> <b>process</b> (2.15) <b>metabo</b> <b>lic</b> <b>process</b> (2.15) <b>cellula</b> <b>r biosynthetic</b> <b>process</b> (1.28)	<b>catalytic</b> <b>activity</b> (2.48) <b>bindin</b> <b>g</b> (2.03) <b>metal ion</b> <b>binding</b> (1.28) <b>ion</b> <b>binding</b> (1.28)

ORF7a protein (QJF77863.1)	<b>methionine (0.90) human (0.88) sars-coronavirus orf7a accessory (0.50) human mterf4-nsun4 (0.50) sars coronavirus orf coded (0.50) chimeric (0.50) 5-ht1b-bril (0.50) ergotamine psi community (0.50)</b>	<b>cell (2.79) cell part (2.79) macromolecular complex (1.62) cytoplasm (1.57)</b>	<b>cellular process (2.72) metabolic process (2.32) macromolecule metabolic process (1.93) biopolymer metabolic process (1.93)</b>	<b>binding (3.78) catalytic activity (2.43) metal ion binding (1.92) ion binding (1.92)</b>
ORF7b protein (QJF77864.1)	<b>domain (1.21) biosynthesis (1.19) human (0.84) phenazine biosynthesis (0.76) stearyl-acyl carrier (0.70) desaturase (0.70) castor seeds (0.70) 76a (0.50)</b>	<b>cell (0.90) cell part (0.90) protein farnesyltransferase complex (0.50) intracellular (0.50)</b>	<b>cellular process (1.26) metabolic process (0.89) biological regulation (0.87) protein farnesylation (0.50)</b>	<b>binding (1.63) metal ion binding (1.26) catalytic activity (1.26) ion binding (1.26)</b>
ORF8 protein (QJF77865.1)	<b>domain (1.98) receptor (1.33) cell (1.00) cerevisiae (0.86) n-terminal (0.80) human (0.78) malt1 (0.53) malt1 paracaspase p21 form (0.50)</b>	<b>cell (2.70) cell part (2.70) cytoplasm (1.47) intracellular (1.47)</b>	<b>cellular process (1.95) localization (1.57) metabolic process (1.55) establishment of localization (1.23)</b>	<b>binding (1.85) protein binding (1.57) catalytic activity (1.44) transferase activity (0.90)</b>
Nucleocapsid phosphoprotein (QJF77866.1)	<b>domain (3.83) nucleocapsid (2.44) coronavirus nucleocapsid (1.75) dimerization domain (1.74) ubiquitin (1.03) human (0.91) oligomerization domain sars coronavirus (0.90) domain sars coronavirus nucleocapsid (0.90)</b>	<b>cytoplasm (0.50) cell (0.50) cell part (0.50) intracellular (0.50)</b>	<b>cellular process (0.83) cellular metabolic process (0.83) cellular biosynthetic process (0.83) metabolic process (0.83)</b>	<b>metal ion binding (1.19) binding (1.19) ion binding (1.19) cation binding (1.19)</b>
ORF10 protein (QJF77867.1)	<b>domain (2.03) human (1.24) isomerase domain (1.00) domain human (0.90) angstrom (0.80) synthase (0.50) xylose isomerase domain (0.50) planctomyces limnophilus (0.50)</b>	<b>cell (3.03) cell part (3.03) intracellular (2.61) intracellular part (2.61)</b>	<b>metabolic process (4.32) cellular process (3.61) cellular metabolic process (3.61) primary metabolic process (2.80)</b>	<b>binding (4.46) catalytic activity (3.96) metal ion binding (2.89) ion binding (2.89)</b>

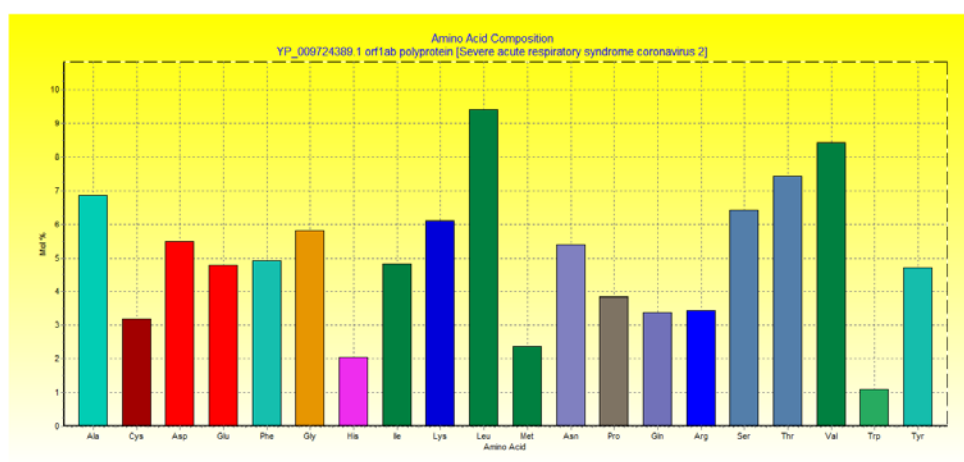


**Figure 2 (A).** Amino acid composition of ORF 1ab protein

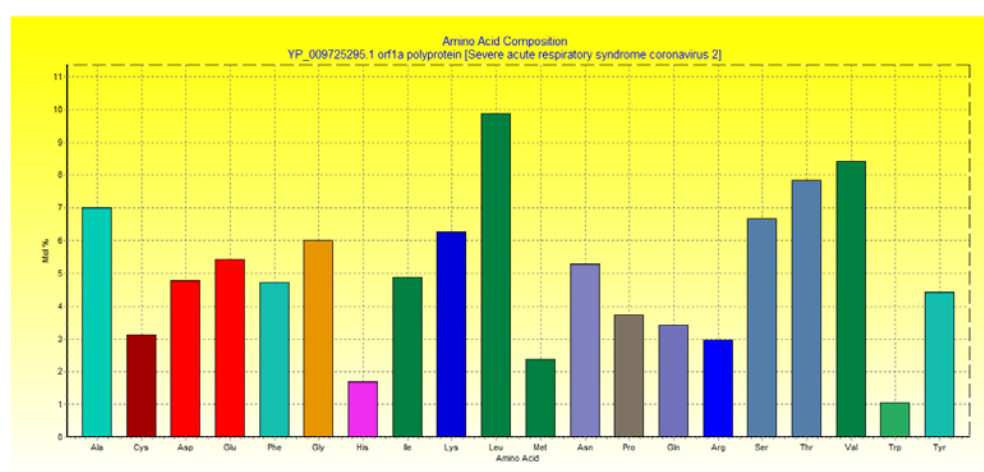


**Figure 2 (B).** Amino acid composition of ORF 1a Protein

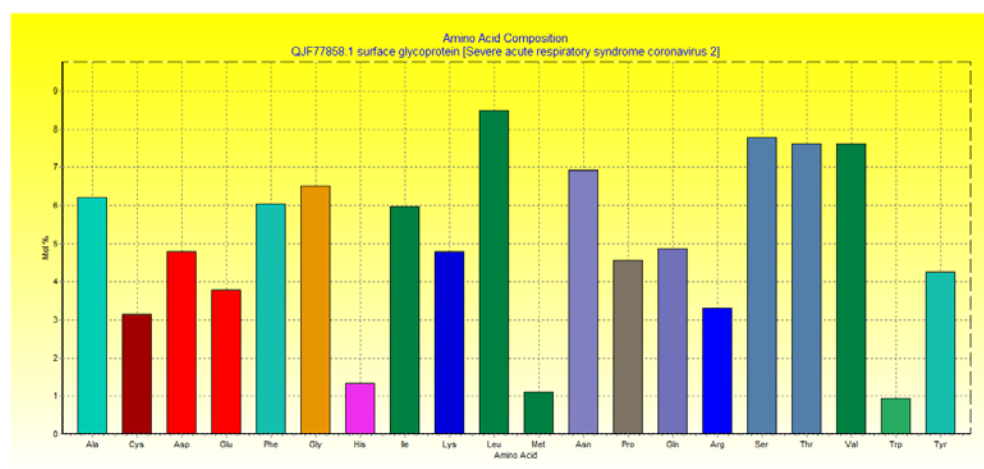


**Figure 2 (C).** Amino acid composition of Surface glycoprotein



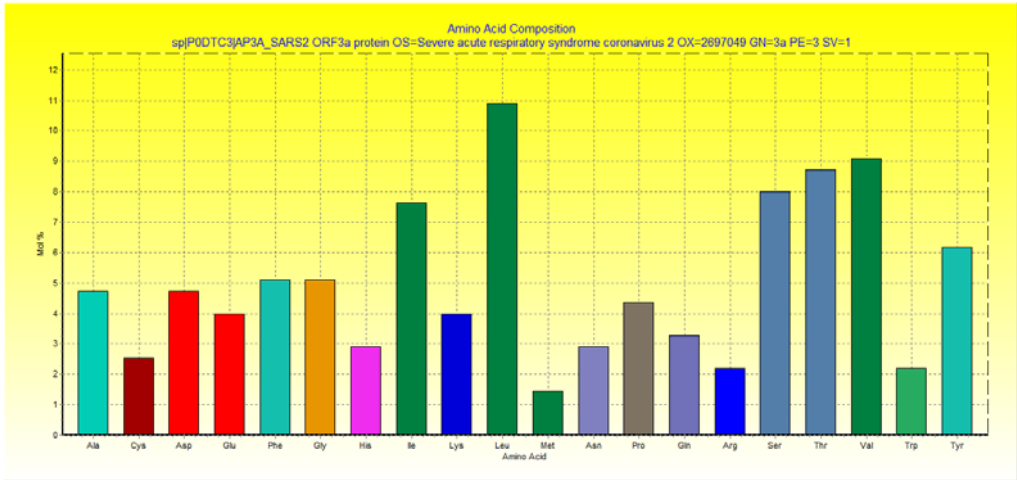


Figure 2 (D). Amino acid composition of ORF 3a protein

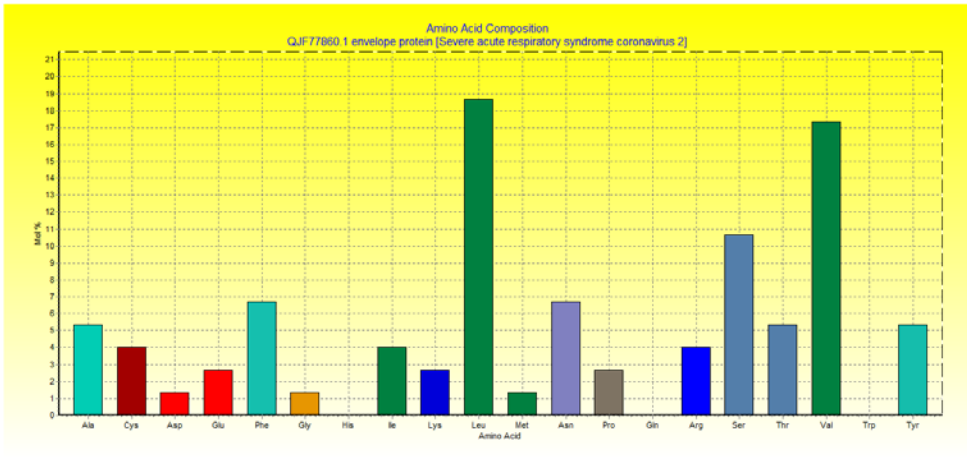


Figure 2 (E). Amino acid composition of Envelope protein

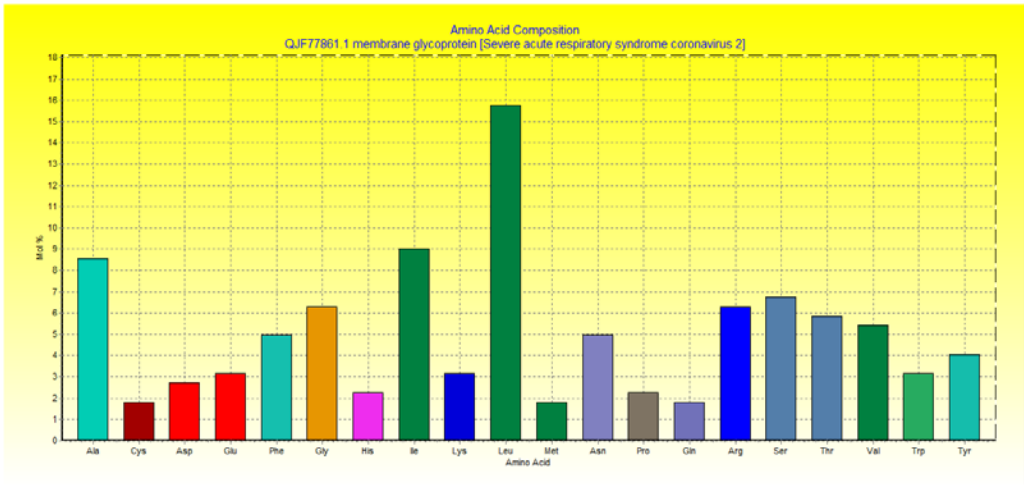
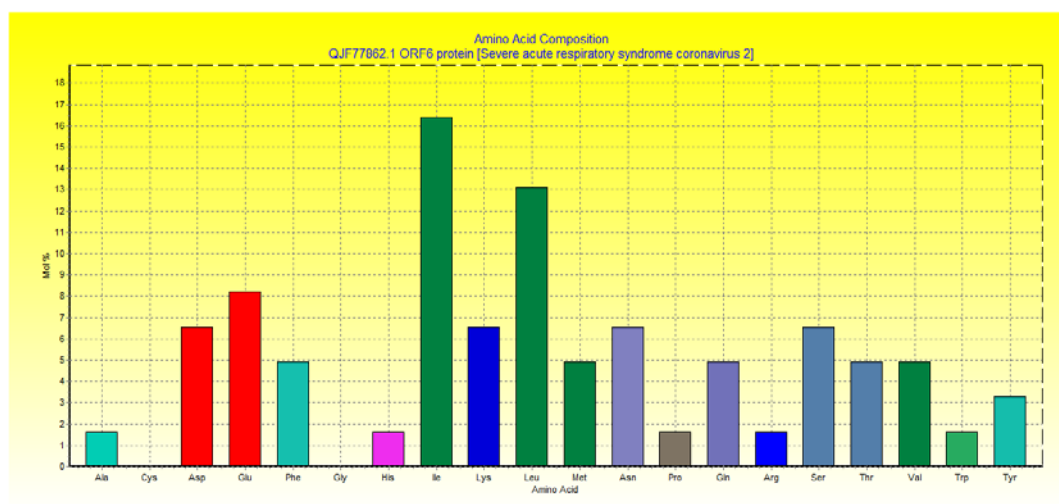
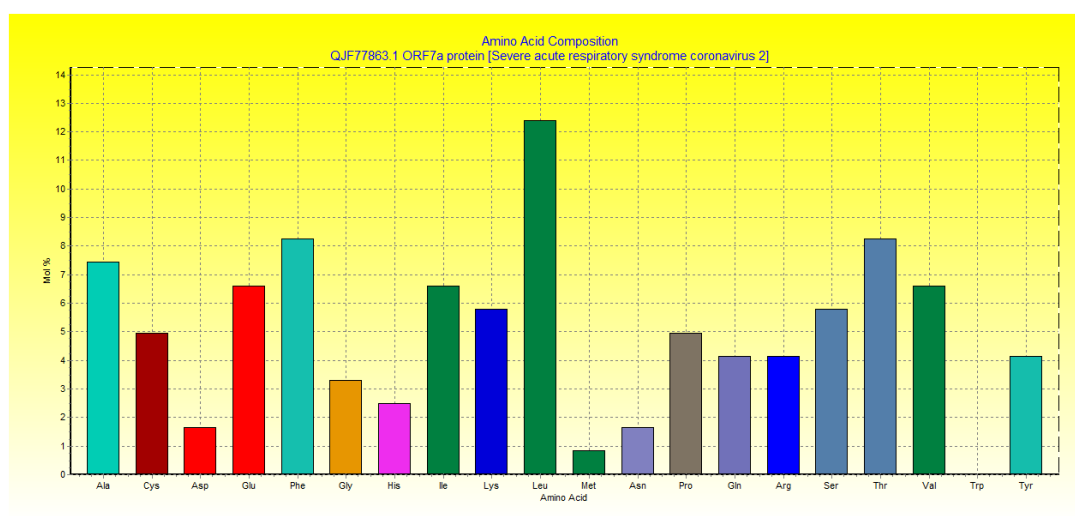


Figure 2 (F). Amino acid composition of Membrane glycoprotein



**Figure 2 (G).** Amino acid composition of ORF6 protein



**Figure 2 (H).** Amino acid composition of ORF 7a protein

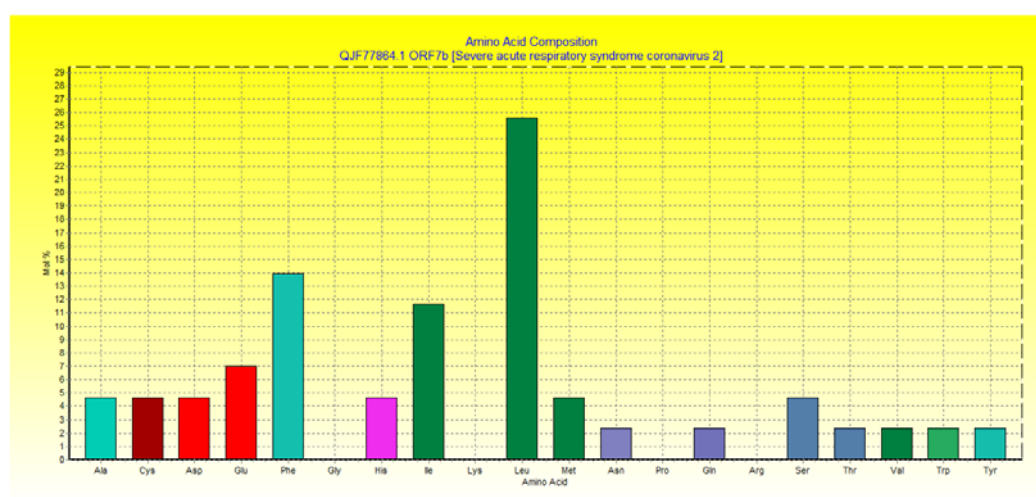


**Figure 2 (I).** Amino acid composition of ORF7b protein

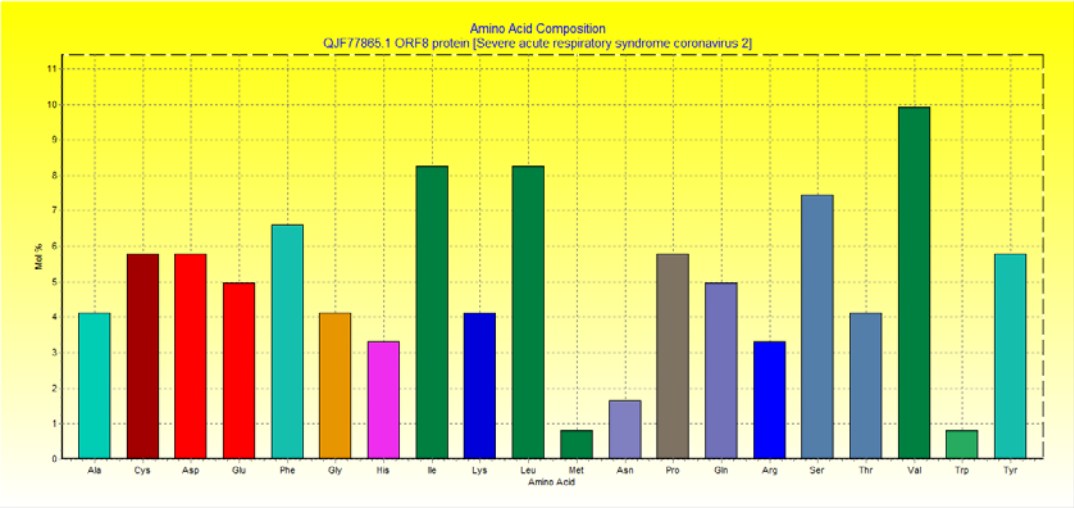


Figure 2 (J). Amino acid composition of ORF8 protein

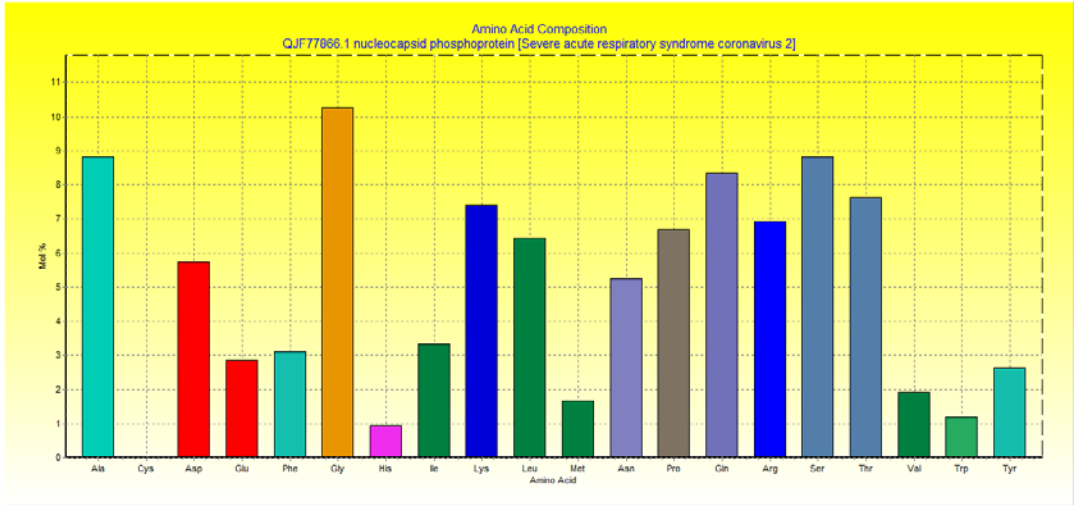


Figure 2 (K). Amino acid composition of Nucleocapsid phosphoprotein

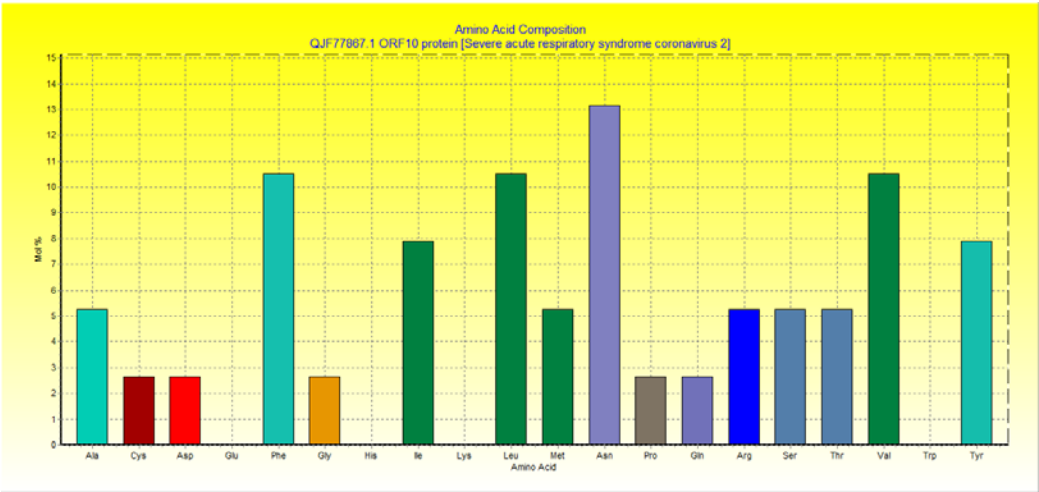
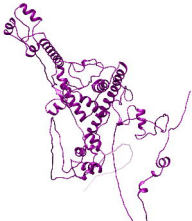
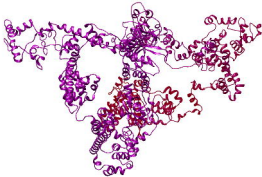


Figure 2 (L). Amino acid composition of ORF10 protein

Figure 2 (A-L). Amino acid distribution histogram for 12 mjr proteins of SARS-CoV-2 proteome

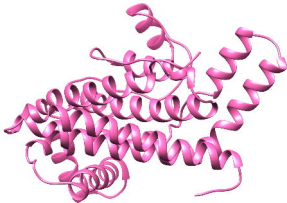


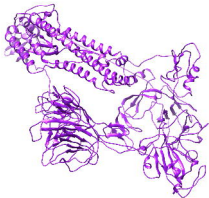


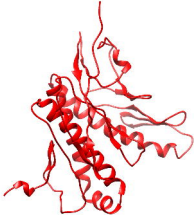


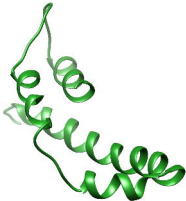






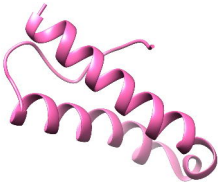




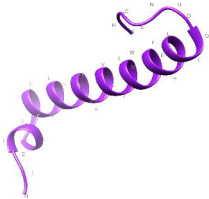


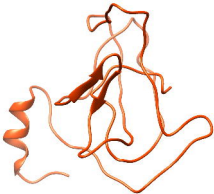




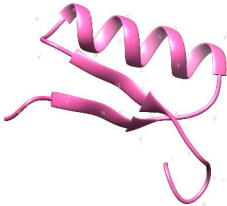














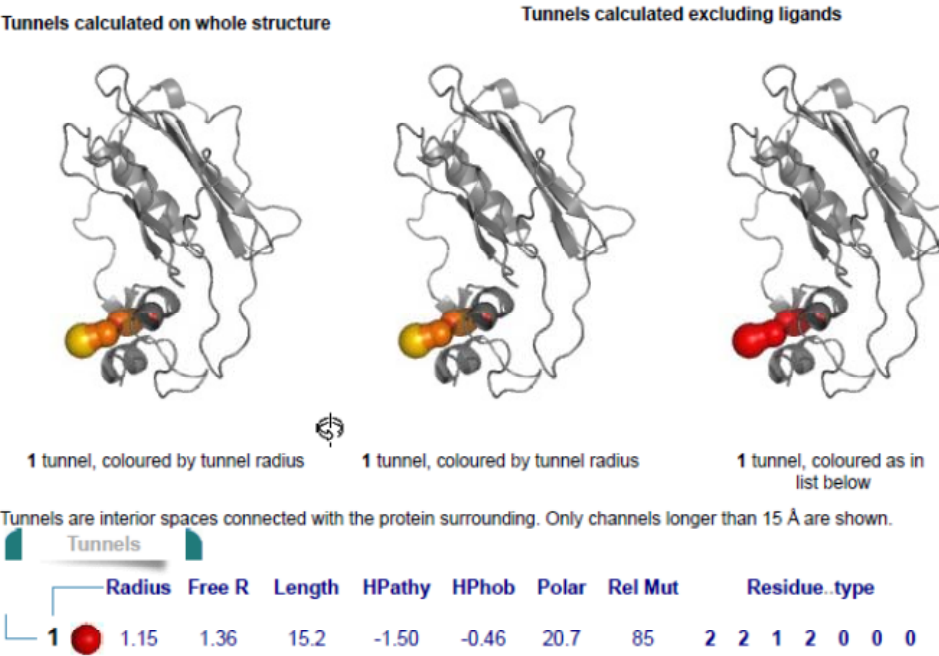


Figure 4 A. NSP1 protein

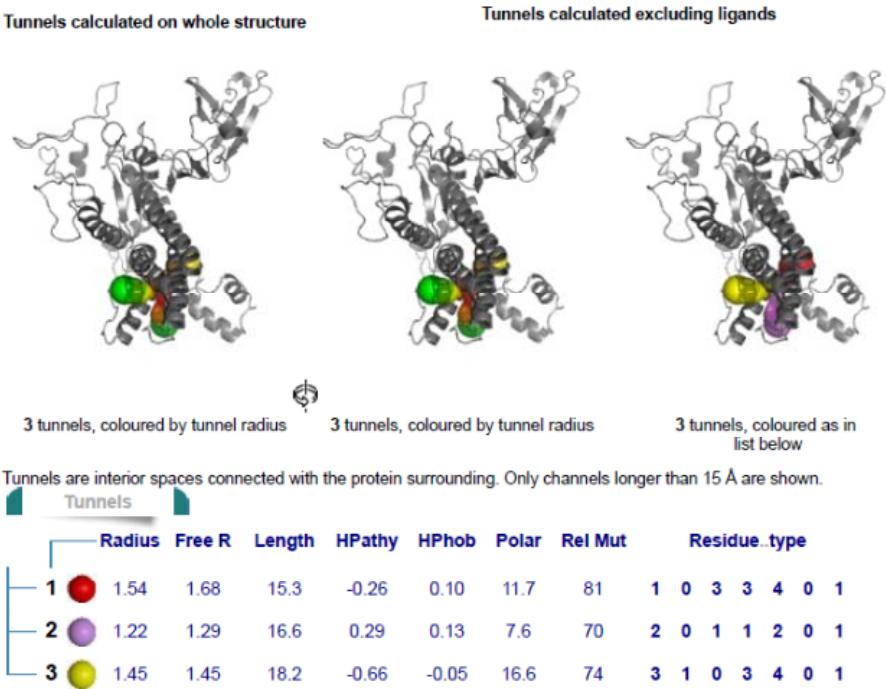


Figure 4 B. NSP 4

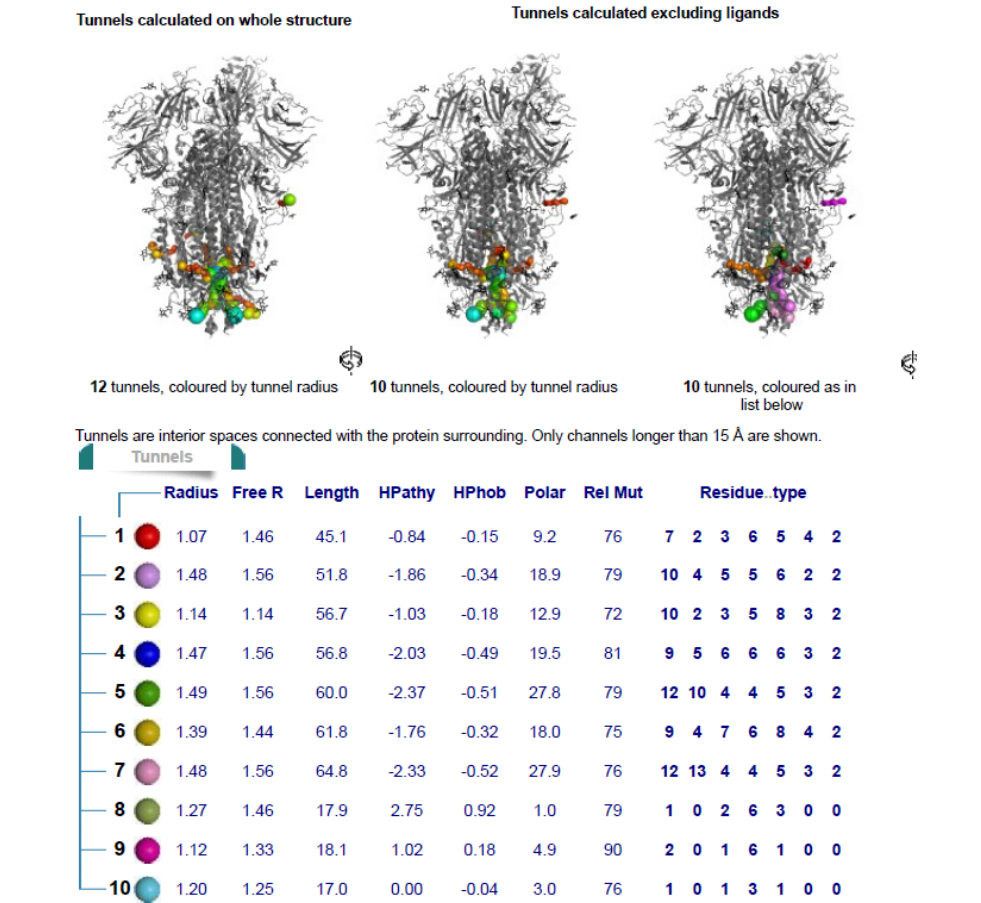


Figure 4 C. Surface glycoprotein.

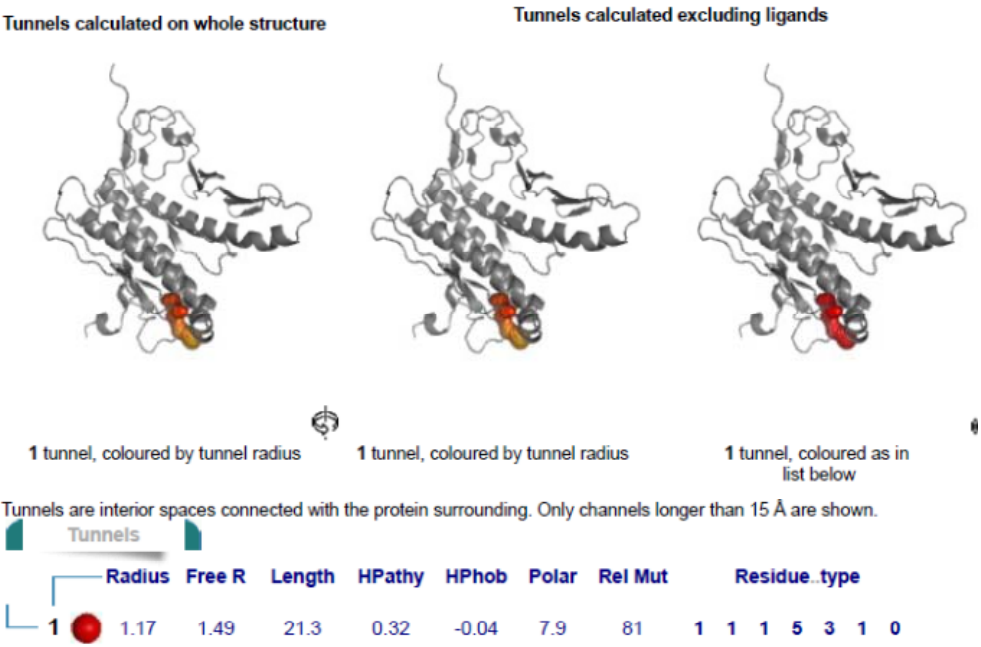


Figure 4 D. ORF 3a protein

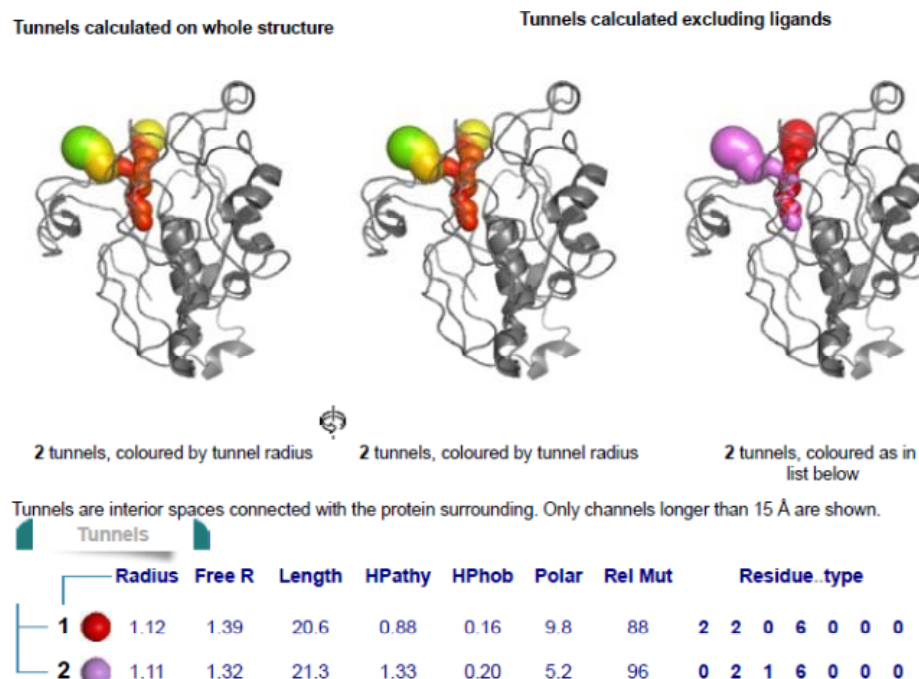


Figure 4 E. Membrane glycoprotein

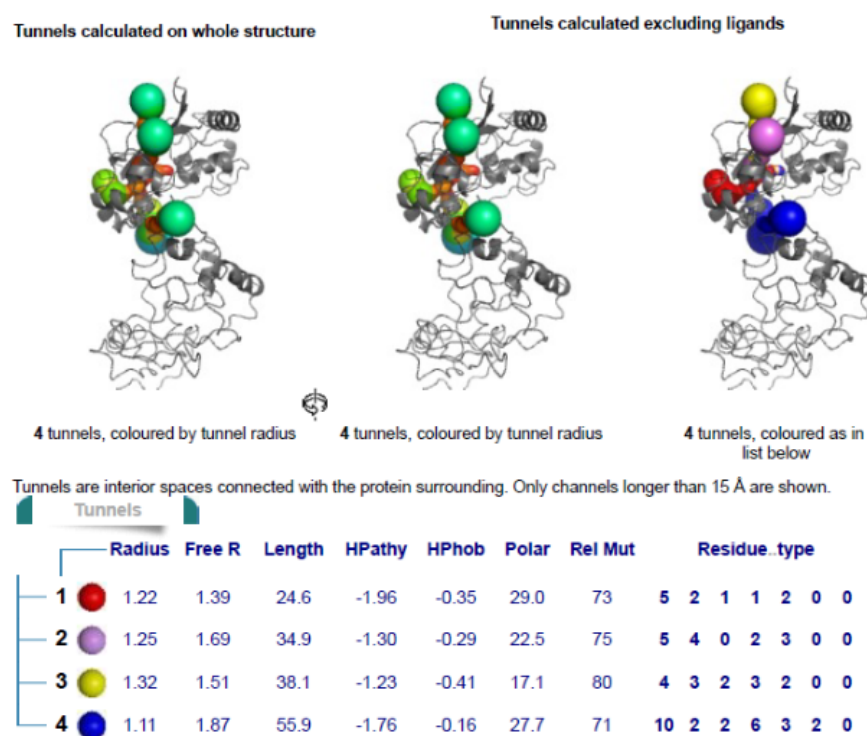
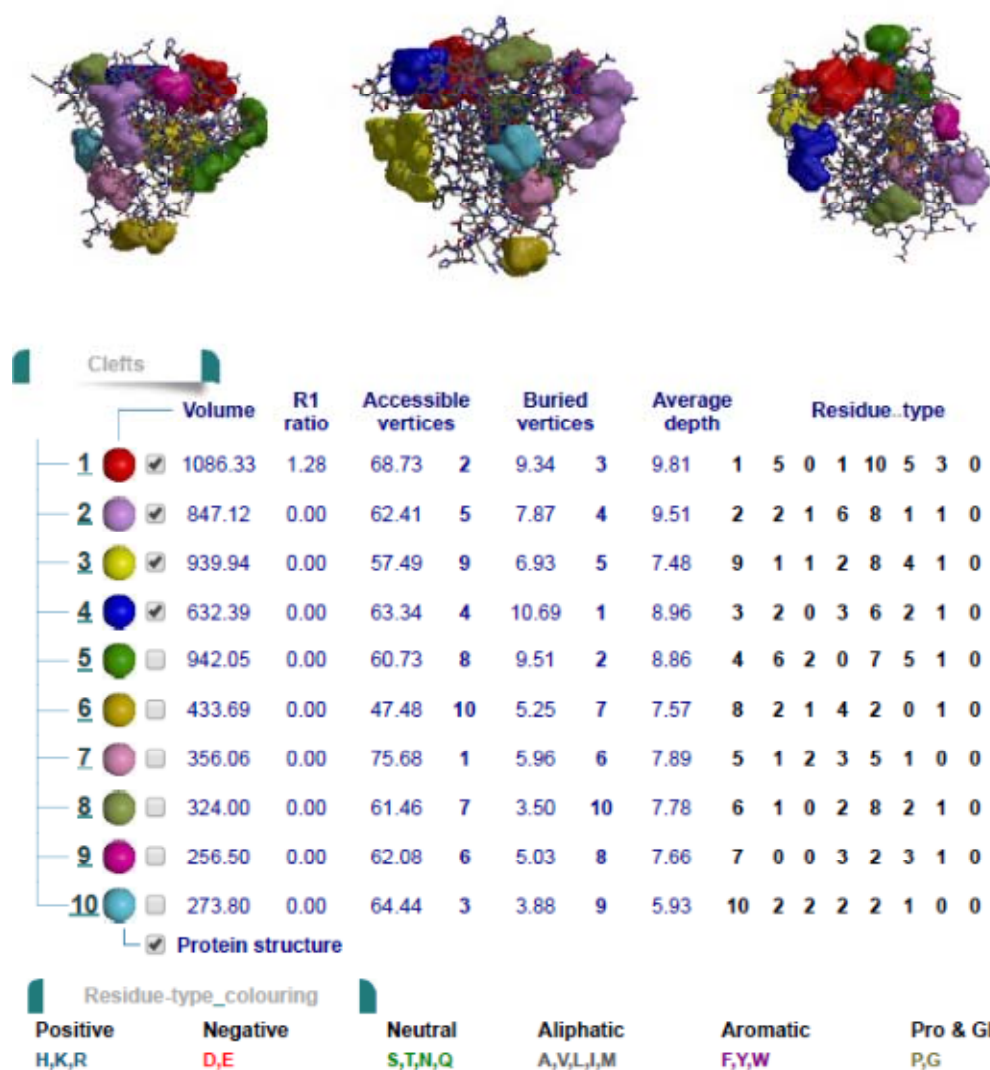
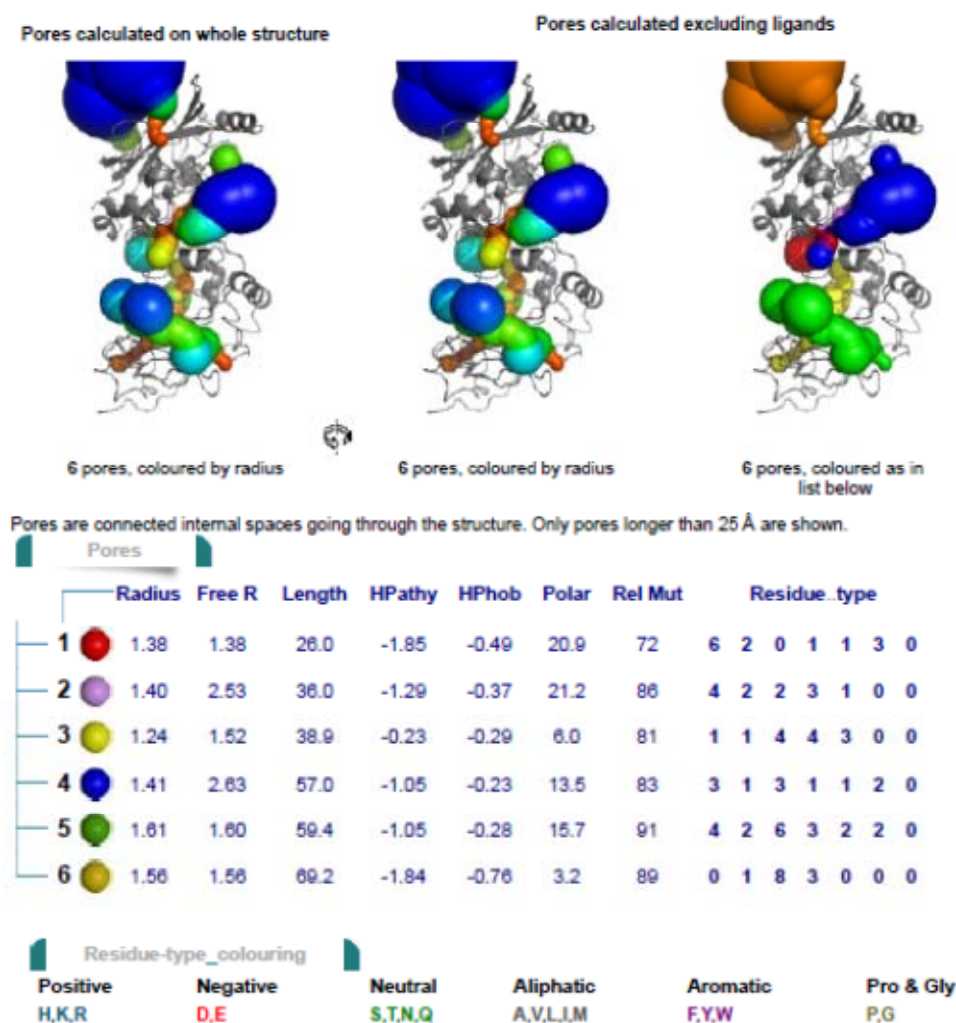


Figure 4 F. Nucleocapsid phosphoprotein

**Figure 4 (A-F).** Tunnels were calculated by **MOLE 2.0 program** version 2.5.13.11.08 and visualized using **Pymol 0.97rc**.



**Figure 5 (A).** Clefts for SARS-COV-2 membrane protein calculated by MOLE 2.0 program version 2.5.13.11.08 and visualized using PyMol 0.97rc.



**Figure 5 (B).** Pores for SARS-COV-2 Nucleocapsis phosphorprotein calculated by MOLE 2.0 program version 2.5.13.11.08 and visualized using Pymol 0.97rc.